Fermi National Accelerator Laboratory

SUSSEX-AST 93/3-1
FERMILAB-PUB-93/029-A
March 1993

Reconstructing the inflaton potential— in principle and in practice

Edmund J. Copeland[1]
School of Mathematical and Physical Sciences,
University of Sussex, Brighton BN1 9QH, U. K.

Edward W. Kolb[2]
NASA/Fermilab Astrophysics Center
Fermi National Accelerator Laboratory, Batavia, IL 60510, and
Department of Astronomy and Astrophysics, Enrico Fermi Institute
The University of Chicago, Chicago, IL 60637

Andrew R. Liddle[3]
Astronomy Centre, School of Mathematical and Physical Sciences,
University of Sussex, Brighton BN1 9QH, U. K.

James E. Lidsey[4]
Astronomy Unit, School of Mathematical Sciences,
Queen Mary and Westfield College, Mile End Road, London E1 4NS, U. K., and
NASA/Fermilab Astrophysics Center
Fermi National Accelerator Laboratory, Batavia, IL 60510

Generalizing the original work by Hodges and Blumenthal, we outline a formalism which allows one, *in principle*, to reconstruct the potential of the inflaton field from knowledge of the tensor gravitational wave spectrum or the scalar density fluctuation spectrum, with special emphasis on the importance of the tensor spectrum. We provide some illustrative examples of such reconstruction. We then discuss in some detail the question of whether one can use real observations to carry out this procedure. We conclude that *in practice*, a full reconstruction of the functional form of the potential will not be possible within the foreseeable future. However, with a knowledge of the dark matter components, it should soon be possible to combine intermediate-scale data with measurements of large-scale cosmic microwave background anisotropies to yield useful information regarding the potential.

PACS number(s): 98.80.-k, 98.80.Cq, 12.10.Dm

email: [1]edmundjc@central.sussex.ac.uk; [2]rocky@fnas01.fnal.gov;
[3]arl@starlink.sussex.ac.uk; [4]jim@fnas09.fnal.gov

Operated by Universities Research Association Inc. under contract with the United States Department of Energy

I. INTRODUCTION

The detection by the *COBE* DMR instrument of fluctuations in the temperature distribution of the Cosmic Microwave Background Radiation (CMBR) on large angular scales [1] is certainly one of the most significant cosmological results since the detection of the CMBR itself. These fluctuations provide valuable information about the nature of primordial perturbations believed responsible for the origin of structure in the Universe. The horizon radius at the epoch of last scattering of the CMBR corresponds to angular scales of about 2° on the sky, which implies that fluctuations on scales probed by *COBE* were not predominantly affected by causal processes or the nature of the matter constituents of the Universe at the time of last scattering of the CMBR. Indeed, the large-scale (greater than 2°) fluctuations arise from the Sachs–Wolfe effect when photons are either red or blue shifted as they climb out of, or fall into, gravitational potential wells [2]. It is most likely that the fluctuations in the CMBR are the result of processes that occurred very early in the history of the Universe, so they yield vital information concerning the physics that led to the primordial perturbations.

There are currently two very attractive scenarios for the origin of the primordial fluctuations: quantum effects during inflation, and gravitational effects of defects resulting from cosmological phase transitions. Both scenarios involve physics beyond the standard model of particle physics, involving energies in the range $10^{10}\text{GeV} \lesssim E \lesssim 10^{19}\text{GeV}$, an energy scale we will refer to loosely as the Grand Unified Theory (GUT) scale. A major difference in the predictions of the two scenarios concern the Gaussian nature of the fluctuation pattern, and we should be able to use this to differentiate between the two possibilities in the near future. In this paper we will assume that the fluctuations are the result of inflation, and we discuss what might be learned about particle physics at very high energies from astronomical observations from which we can infer the primordial fluctuation spectrum.

All models of inflation involve a period of rapid growth of the size of the Universe. This is most easily illustrated by considering a homogeneous, isotropic Universe with a flat Friedmann–Robertson–Walker (FRW) metric described in term of a scale factor $a(t)$. Here, "rapid growth" means a positive value of $\ddot{a}/a = -(4\pi G_N/3)(\rho+3p)$ where ρ is the energy density and p the pressure. In all successful models of inflation, the Universe is dominated by some sort of scalar "potential" energy density $V > 0$ that is positive, resulting in an effective equation of state $\rho \simeq -p \simeq V$, and hence $\ddot{a} > 0$. If one identifies the potential energy as arising from the potential of some scalar field ϕ, then ϕ is known as the *inflaton* field.

Even within this traditional view of inflation, there are two major ways to implement the scenario. One way involves a first-order phase transition. In this method, either in the original proposal of Guth [3] or the latest version called extended inflation [4], the inflaton is trapped in a meta-stable, or false-vacuum, state while the Universe inflates. Inflation is ended when the Universe undergoes a first-order phase

transition in which the inflaton field tunnels to its true-vacuum state. In the second method, inflation occurs because for some reason the inflaton field is displaced from its minimum and its potential energy density dominates the Universe; inflation occurs while the inflaton field is slowly evolving, or rolling, to its minimum [5, 6]. It is this second class of "slow-roll" models we will consider in this paper.[1]

Although the early slow-roll models had potentials that were reasonably simple (Coleman–Weinberg, $\lambda\phi^4$, etc.), or at least polynomials in some scalar field, many attractive models have been developed where the scalar potential driving inflation is quite complicated. Perhaps the study of the density perturbations produced by inflation can shed some light on the nature of the potential.

Broadly speaking, inflation predicts a very nearly Gaussian spectrum of density perturbations that is *scale dependent*, i.e., the amplitude of the perturbation depends upon the length scale. Such a dependence typically arises because the Hubble expansion rate during the inflationary epoch in fact changes, albeit slowly, as the field driving the expansion rolls towards the minimum of the scalar potential. This implies that the amplitude of the fluctuations as they cross the Hubble radius will be weakly time-dependent.

Within the context of slow-roll inflation, Hodges and Blumenthal [7] have shown that any scale dependence for density perturbations is possible if one considers an arbitrary functional form for the inflaton potential, $V(\phi)$. In this sense, inflation makes no unique prediction concerning the form of the spectrum and one is left with two options. Either one can aim to find a deeper physical principle that uniquely determines the potential, or observations that depend on $V(\phi)$ can be employed to limit the number of possibilities.

Improved observations of large-scale structure, of which *COBE* provides the most dramatic example at present, are important because they allow us, in principle, to determine the spectrum of primordial density perturbations. This may very well provide a direct experimental window on the physics of the Grand Unified era corresponding to energy scales of the order 10^{16} GeV. The purpose of the present work is to investigate to what extent information from the CMBR and large-scale galactic structure will allow us to reconstruct GUT physics.

In the following section we will review the salient aspects of slow-roll inflation. In Section III we discuss the reconstruction of the inflaton potential from knowledge of scalar or tensor perturbations. Section IV illustrates the formalism by several examples in which the functional form of the potential is found from knowledge of the tensor and scalar perturbation spectra. Section V illustrates what can be learned about the potential from observations of the properties of the tensor and scalar spectra at a particular length scale. In Section VI the reader may find a discussion of how one determines the primordial density spectrum. Finally, Section VII offers an assessment of the prospectus for reconstruction of the inflaton potential.

[1] In reality, often the distinction between the two methods is not so clean, and it is possible to consider some types of first-order inflation models as variants of slow-roll models. See Ref. [4].

II. REVIEW OF SLOW-ROLL INFLATION

For the benefit of those not familiar with the generation of scalar and tensor perturbations in slow-roll inflation, we review the salient features in this section. Those comfortable with the basic results may wish to skip this section, and refer back to it as needed to understand notation and conventions. We set $c = \hbar = 1$, and define $\kappa^2 = 8\pi G_N = 8\pi/m_{Pl}^2$.

Slow-roll inflation requires a scalar field ϕ to be displaced from the minimum of its potential at some time early in the evolution of the Universe. If during the evolution of the field to its minimum a region of the Universe is dominated by the potential energy of the field, then the volume of that region will undergo rapid expansion, inflate, and grow to encompass a volume large enough to contain all of the presently observed Universe. Eventually the potential energy ceases to dominate when the field evolves through a steep region of the potential and the field evolves so rapidly that the kinetic energy of the field comes to dominate. This is the end of inflation, and is followed by the scalar field oscillating about the minimum of its potential, with the inflaton field decaying and 're-heating' the Universe by conversion of vacuum energy to radiation.

We are interested in the perturbations resulting from inflation. The "density" perturbations are usually described in term of fluctuations in the local value of the mass density. In a Universe with density field $\rho(\mathbf{x})$ and mean mass density ρ_0, the density contrast is defined as

$$\delta(\mathbf{x}) = \frac{\delta\rho(\mathbf{x})}{\rho_0} = \frac{\rho(\mathbf{x}) - \rho_0}{\rho_0}. \tag{2.1}$$

It is convenient to express this contrast in terms of a Fourier expansion:

$$\delta(\mathbf{x}) = A \int \delta_{\mathbf{k}} \exp(-i\mathbf{k}\cdot\mathbf{x}) d^3k, \tag{2.2}$$

where A is simply some overall normalization constant, interesting only for those who enjoy keeping track of factors of 2π. What is usually meant by the density perturbation on a scale λ, $(\delta\rho/\rho)_\lambda$, is related to the square of the Fourier coefficients $\delta_{\mathbf{k}}$:

$$\left(\frac{\delta\rho}{\rho}\right)_\lambda^2 \equiv A' \frac{k^3|\delta_k|^2}{2\pi^2}\bigg|_{\lambda=k^{-1}}, \tag{2.3}$$

where again we have included an overall normalization constant A'. The perturbations are normally taken to be (statistically) isotropic, in the sense that the expectation of $|\delta_{\mathbf{k}}|^2$ averaged over a large number of independent regions can depend only on $k = |\mathbf{k}|$. The dependence of $\delta\rho/\rho$ as a function of λ is the spectrum of the density perturbations. Of crucial importance is the relative size of scale λ to the scale of the Hubble radius. The *physical* length between two points of coordinate separation d is

$\lambda(t) = a(t)d$. A length scale comoving with the expansion will grow proportional to $a(t)$. If $\ddot{a}(t) < 0$, as in the standard non-inflationary phase, then $a(t)$ will grow slower than t. If $\ddot{a}(t) > 0$, as in the inflationary phase, then $a(t)$ will grow faster than t.

For a spatially flat isotropic Universe the Hubble expansion rate, $H(t) = \dot{a}/a$, is given by $3H^2(t) = \kappa^2\rho(t)$. The inverse of the Hubble expansion rate, the Hubble radius $\lambda_H(t) \equiv H^{-1}(t)$, is the scale beyond which causal processes no longer operate. In the non-inflationary phase λ_H increases linearly with time. Since in the non-inflationary phase $\lambda_H \propto t$, while $\lambda(t)$ increases more slowly than t, the Hubble radius increases faster than $\lambda(t)$, and a length scale $\lambda(t)$ will start larger than the Hubble radius ($\lambda > \lambda_H$), cross the Hubble radius ($\lambda = \lambda_H$), and then will remain inside the Hubble radius ($\lambda < \lambda_H$).

The story is different if we imagine that the Universe was once in an inflationary phase. In inflation H is roughly constant, so the Hubble length is roughly time independent. Thus, a given scale can start sub-Hubble radius, $\lambda < \lambda_H$, then pass outside the Hubble radius during inflation, and then re-enter the Hubble radius after inflation. Thus, perturbations can be imparted on a given length scale in the inflationary era as that scale leaves the Hubble radius, and will be present as that scale re-enters the Hubble radius after inflation in the radiation-dominated or matter-dominated eras.

Microphysics cannot affect the perturbation while it is outside the Hubble radius, and the evolution of its amplitude is *kinematical*, unaffected by dissipation, the equation of state, instabilities, and the like. However, for super-Hubble radius sized perturbations one must take into account the freedom in the choice of the background reference space-time, i.e., the gauge ambiguities. As usual when confronted with such a problem, it is convenient to calculate a *gauge-invariant* quantity. For inflation it is convenient to study a quantity conventionally denoted ζ [8]. In the uniform Hubble constant gauge, at Hubble radius crossing ζ is particularly simple, related to the background energy density and pressure ρ_0 and p_0, and the perturbed energy density ρ_1:

$$\zeta \equiv \delta\rho/(\rho_0 + p_0), \tag{2.4}$$

where $\delta\rho = \rho_1 - \rho_0$ is the density perturbation.

In the standard matter-dominated (MD) or radiation-dominated (RD) phase, ζ at Hubble radius crossing (up to a factor of order unity) is equal to $\delta\rho/\rho$. Thus, the amplitude of a density perturbation when it crosses back inside the Hubble radius after inflation, $(\delta\rho/\rho)_{\rm HOR}$,[2] is given by ζ at the time the fluctuation crossed outside the Hubble radius during inflation.

As inferred from the adoption of ζ, the convenient specification of the amplitude of density perturbations on a particular scale is when that particular scale just enters the Hubble radius, denoted as $(\delta\rho/\rho)_{\rm HOR}$. Specifying the amplitude of the perturbation at Hubble radius crossing evades the subtleties associated with the gauge freedom,

[2]The notation "HOR" follows because often in the literature the Hubble radius is referred to (incorrectly) as the horizon.

and has the simple Newtonian interpretation as the amplitude of the perturbation in the gravitational potential. Of course, when one specifies the fluctuation spectrum at Hubble radius crossing, the amplitudes for different lengths are specified at *different* times.

Now let us turn to the scalar field dynamics during inflation. Consider a minimally coupled, spatially homogeneous scalar field ϕ, with Lagrangian density

$$\mathcal{L} = \partial^\mu \phi \partial_\mu \phi/2 - V(\phi) = \dot{\phi}^2/2 - V(\phi). \tag{2.5}$$

With the assumption that ϕ is spatially homogeneous, the stress-energy tensor takes the form of a perfect fluid, with energy density and pressure given by $\rho_\phi = \dot{\phi}^2/2 + V(\phi)$, and $p_\phi = \dot{\phi}^2/2 - V(\phi)$. The classical equation of motion for ϕ is

$$\ddot{\phi} + 3H\dot{\phi} + V'(\phi) = 0, \tag{2.6}$$

with the expansion rate in a flat FRW spacetime given by

$$H^2 = \frac{\kappa^2}{3}\left(\frac{1}{2}\dot{\phi}^2 + V(\phi)\right). \tag{2.7}$$

Here dot and prime denote differentiation with respect to cosmic time and ϕ respectively. We assume that inflation has already provided us with a flat universe by the time the largest observable scales cross the Hubble radius.

By differentiating Eq. (2.7) with respect to t and substituting in Eq. (2.6), we arrive at the "momentum" equation

$$2\dot{H} = -\kappa^2 \dot{\phi}^2. \tag{2.8}$$

All minimal slow-roll models are examples of sub-inflationary behavior, which is defined by the condition $\dot{H} < 0$. Super-inflation, where $\dot{H} > 0$, cannot occur here, though it is possible in more complex scenarios [9, 10]. We may divide both sides of this equation by $\dot{\phi}$ if this quantity does not pass through zero. This allows us to eliminate the time-dependence in the Friedmann equation [Eq. (2.7)] and derive the first-order, non-linear differential equations

$$(H')^2 - \frac{3}{2}\kappa^2 H^2 = -\frac{1}{2}\kappa^4 V(\phi) \tag{2.9}$$

$$\kappa^2 \dot{\phi} = -2H'. \tag{2.10}$$

A common framework for discussion of inflation is the slow-roll approximation, though let us emphasize here that in much of our treatment of inflaton dynamics we shall not need to resort to it. We can define two parameters, which we will denote as slow-roll parameters, by[3]

$$\epsilon \equiv \frac{3\dot{\phi}^2}{2}\left(V + \frac{\dot{\phi}^2}{2}\right)^{-1} = \frac{2}{\kappa^2}\left(\frac{H'}{H}\right)^2$$

[3]These definitions differ slightly from, and indeed improve upon, those of Refs. (11), (12) which were made using the potential rather than the Hubble parameter. As defined here they possess rather more elegant properties.

$$\eta \equiv \frac{\ddot{\phi}}{H\dot{\phi}} = \frac{2}{\kappa^2}\frac{H''}{H}. \tag{2.11}$$

Slow-roll corresponds to $\{\epsilon, |\eta|\} \ll 1$. These conditions correspond respectively to the cases when the first term in Eq. (2.9) and the first term in its ϕ-derivative can be neglected.

With these definitions, the end of inflation is given *exactly*[4] by $\epsilon = 1$. A small value of η guarantees

$$3H\dot{\phi} \simeq -V'(\phi), \tag{2.12}$$

which is often called the slow-roll equation.[5] Although the terminology "slow-roll approximation" is normally used rather loosely, one could imagine carrying out a formalized perturbation expansion in the slow-roll parameters, and we shall refer to such results later.

Density perturbations arise as the result of quantum-mechanical fluctuations of fields in de Sitter space. First, let's consider scalar density fluctuations. To a good approximation we may treat the inflaton field ϕ as a massless, minimally coupled field. (Of course the inflaton does have a mass, but inflation operates when the field is evolving through a "flat" region of the potential.) Just as fluctuations in the density field may be expanded in a Fourier series as in Eq. (2.1), the fluctuations in the inflaton field may be expanded in terms of its Fourier coefficients $\delta\phi_{\mathbf{k}}$: $\delta\phi(\mathbf{x}) \propto \int \delta\phi_{\mathbf{k}} \exp(-i\mathbf{k}\cdot\mathbf{x}) d^3k$. During inflation there is an event horizon as in de Sitter space, and quantum-mechanical fluctuations in the Fourier components of the inflaton field are given by [13]

$$k^3 |\delta\phi_{\mathbf{k}}|^2 / 2\pi^2 = (H/2\pi)^2, \tag{2.13}$$

where $H/2\pi$ plays a role similar to the Hawking temperature of black holes. Thus, when a given mode of the inflaton field leaves the Hubble radius during inflation, it has impressed upon it quantum mechanical fluctuations. In analogy to Eq. (2.3), what is called the fluctuations in the inflaton field on scale k is proportional to $k^{3/2}|\delta\phi_{\mathbf{k}}|$, which by Eq. (2.13) is proportional to $H/2\pi$. Fluctuations in ϕ lead to perturbations in the energy density:

$$\delta\rho_\phi = \delta\phi(\partial V/\partial\phi). \tag{2.14}$$

Now considering the fluctuations as a particular mode leaves the Hubble radius during inflation, we may construct the gauge invariant quantity ζ from Eq. (2.4) using the fact that during inflation $\rho_0 + p_0 = \dot{\phi}^2$:

$$\zeta = \delta\phi \left(\frac{\partial V}{\partial\phi}\right) \frac{1}{\dot{\phi}^2}. \tag{2.15}$$

[4] With the definition of ϵ in Refs. (11), (12), this result is true only in the slow-roll approximation.

[5] Note the difference between slow-roll inflation and the slow-roll equation. Slow-roll inflation is a model where inflation occurs where the scalar field is slowly evolving to its minimum, while the slow-roll equation implies that $\ddot{\phi}$ can be neglected.

Now using Eq. (2.9) and Eq. (2.10), the amplitude of the density perturbation when it crosses the Hubble radius *after* inflation is

$$\left(\frac{\delta\rho}{\rho}\right)_\lambda^{\rm HOR} \equiv \frac{m}{\sqrt{2}} A_S(\phi) = \frac{m\kappa^2}{8\pi^{3/2}} \frac{H^2(\phi)}{|H'(\phi)|} \propto \frac{V^{3/2}(\phi)}{m_{Pl}^3 V'(\phi)}, \tag{2.16}$$

where $H(\phi)$ and $H'(\phi)$ are to be evaluated when the scale λ crossed the Hubble radius *during* inflation. The constant m equals 2/5 or 4 if the perturbation re-enters during the matter or radiation dominated eras respectively.[6] Now we wish to know the λ-dependence of $(\delta\rho/\rho)_\lambda$, while the right-hand side of the equation is a function of ϕ when λ crossed the Hubble radius during inflation. We may find the value of the scalar field when the scale λ goes outside the Hubble radius in terms of the number of e-foldings of growth in the scale factor between Hubble radius crossing and the end of inflation.

It is quite a simple matter to calculate the number of e-foldings of growth in the scale factor that occur as the scalar field rolls from a particular value ϕ to the end of inflation ϕ_e:

$$N(\phi) \equiv \int_{te}^{t} H(t')dt' = -\frac{\kappa^2}{2}\int_{\phi}^{\phi_e} \frac{H(\phi')}{H'(\phi')} d\phi'. \tag{2.17}$$

The slow-roll conditions guarantee a large number of e-foldings. The total amount of inflation is given by $N_{\rm TOT} \equiv N(\phi_i)$, where ϕ_i is the initial value of ϕ at the start of inflation (when $\ddot{a}$ first becomes positive). In general, the number of e-folds between when a length scale λ crossed the Hubble radius during inflation and the end of inflation is given by [11]

$$N(\lambda) = 45 + \ln(\lambda/{\rm Mpc}) + \frac{2}{3}\ln(M/10^{14}\,{\rm GeV}) + \frac{1}{3}\ln(T_{\rm RH}/10^{10}\,{\rm GeV}), \tag{2.18}$$

where M is the mass scale associated with the potential and $T_{\rm RH}$ is the "re-heat" temperature. Relating $N(\lambda)$ and $N(\phi)$ from Eq. (2.17) results in an expression between ϕ and λ. Hopefully this dry formalism will become clear in the example discussed below.

In addition to the scalar density perturbations caused by de Sitter fluctuations in the inflaton field, there are gravitational mode perturbations, $g_{\mu\nu} \rightarrow g_{\mu\nu}^{\rm FRW} + h_{\mu\nu}$, caused by de Sitter fluctuations in the metric tensor [14,15]. Here, $g_{\mu\nu}^{\rm FRW}$ is the Friedmann–Robertson–Walker metric and $h_{\mu\nu}$ are the metric perturbations. That de Sitter space fluctuations should lead to fluctuations in the metric tensor is not surprising, since after all, gravitons are the propagating modes associated with transverse, traceless metric perturbations, and they too behave as minimally coupled scalar

[6] The 4 for radiation is appropriate to the uniform Hubble constant gauge. One occasionally sees a value 4/9 instead which is appropriate to the synchronous gauge. The matter domination factor is the same in either case. Note also that it is exact for matter domination, but for radiation domination it is only strictly true for modes much larger than the Hubble radius, and there will be corrections in the extrapolation down to the size of the Hubble radius.

fields. The dimensionless tensor metric perturbations can be expressed in terms of two graviton modes we will denote as h. Performing a Fourier decomposition of h, $h(\vec{x}) \propto \int \delta h_k \exp(-i\vec{k}\cdot\vec{x}) d^3k$, we can use the formalism for scalar field perturbations simply by the identification $\delta\phi_{\mathbf{k}} \rightarrow h_{\mathbf{k}}/\kappa\sqrt{2}$, with resulting quantum fluctuations [cf. Eq. (2.13)]

$$k^3|h_{\mathbf{k}}|^2/2\pi^2 = 2\kappa^2(H/2\pi)^2. \tag{2.19}$$

While outside the Hubble radius, the amplitude of a given mode remains constant, so the amplitude of the dimensionless strain on scale λ when it crosses the Hubble radius after inflation is given by

$$\left|k^{3/2}h_{\mathbf{k}}\right|_{\lambda}^{\mathrm{HOR}} \equiv A_G(\phi) = \frac{\kappa}{4\pi^{3/2}} H(\phi) \sim \frac{V^{1/2}(\phi)}{m_{Pl}^2}, \tag{2.20}$$

where once again $H(\phi)$ is to be evaluated when the scale λ crossed the Hubble radius *during* inflation.

As usual, it is convenient to illustrate the general features of inflation in the context of the simplest model, chaotic inflation [6], which is to inflationary cosmology what *drosophila* is to genetics. In chaotic inflation the inflaton potential is usually taken to have a simple polynomial form such as $V(\phi) = \lambda\phi^4$, or $V(\phi) = \mu^2\phi^2$. For a concrete example, let us consider the simplest chaotic inflation model, with potential $V(\phi) = \mu^2\phi^2$ [16]. This model can be adequately solved in the slow-roll approximation, yielding

$$\begin{aligned}
\phi(t) &= \phi_i - \frac{2}{\sqrt{3}}\frac{\mu}{\kappa}t \\
a(t) &= a_i \exp\left[\frac{\kappa\mu}{\sqrt{3}}\left(\phi_i t - \frac{\mu}{\sqrt{3}\kappa}t^2\right)\right] \\
H &= \frac{\kappa\mu}{\sqrt{3}}\left(\phi_i - \frac{2}{\sqrt{3}}\frac{\mu}{\kappa}t\right) = \frac{\kappa\mu}{\sqrt{3}}\phi,
\end{aligned} \tag{2.21}$$

with inflation ending at $\kappa\phi_e = \sqrt{2}$ as determined by $\epsilon = 1$, where ϵ was defined in Eq. (2.11). The number of e-foldings between a scalar field value ϕ, and the end of inflation is just

$$N(\phi) = -\frac{\kappa^2}{2}\int_{\phi}^{\sqrt{2}/\kappa} \frac{H(\phi')}{H'(\phi')} d\phi' = \frac{\kappa^2\phi^2}{4} - \frac{1}{2}. \tag{2.22}$$

Equating Eq. (2.22) and Eq. (2.18) relates ϕ and λ in this model for inflation:

$$\kappa^2\phi^2/4 = [45.5 + \ln(\lambda/\mathrm{Mpc})]. \tag{2.23}$$

Using Eq. (2.16) and Eq. (2.20), A_S and A_G are found to be

$$\begin{aligned}
A_S(\lambda) &= \left(\sqrt{2}\kappa\mu/\sqrt{12\pi^3}\right)[45.5 + \ln(\lambda/\mathrm{Mpc})] \\
A_G(\lambda) &= \left(\kappa\mu/\sqrt{12\pi^3}\right)[45.5 + \ln(\lambda/\mathrm{Mpc})]^{1/2}.
\end{aligned} \tag{2.24}$$

We can note three features that are common to a large number of (but not all) inflationary models. First, A_S and A_G have different functional dependences upon λ. Second, A_G and A_S increase with λ. Finally, $A_S > A_G$, for scales of interest, although not by an enormous factor.

To conclude this exercise, it is worth reminding the reader how little of the inflaton potential is available for reconstruction. The scales of cosmological interest at the present epoch lie in the range $1h^{-1}$ Mpc for galaxies up to the current horizon size of $6000h^{-1}$ Mpc, where as usual h is Hubble's constant in units of 100 km s^{-1}Mpc^{-1}. Taking the present horizon distance to have crossed the Hubble radius 60 e-foldings from the end of inflation, we see that we only sample the small region of the potential $V(\phi)$ for $\phi \in [2.7m_{Pl}, 3.0m_{Pl}]$. By any standards, the density perturbations from inflation we can actually sample represent an extremely small region of the potential. However it should be realized that although we have potential information about a small region of the potential, any information about the GUT potential, no matter how meager, is precious! Indeed, in the exploration of GUTs, cosmology may reveal the first "piece of the action."

We have one further piece of information, which is that we know that the remainder of inflation must occur in the remaining section of the potential, with the scalar field coming to rest with $V(\phi) = 0$. Although this represents a significant constraint on the potential on scales below those that large-scale structure observations can sample, it does still leave an uncountable infinity of possible forms in this region. (One other constraint in this region comes from primordial black holes, whose abundance can in principle be calculated from the spectrum. Should black hole formation be copious, this constrains the spectrum at the mass scales corresponding to the size of detectable black holes, which are most prominent at around 10^{15}g [17].)

To conclude this section we call the reader's attention to Figure 1, which illustrates the procedure. The figure illustrates a scalar field ϕ rolling down a potential $V(\phi)$. At some point in the evolution the slow-roll conditions break down and inflation ends. We can count back from this point the number of e-foldings from the end of inflation, and use this information to find a relationship between the value of ϕ in the evolution, and the length scale λ leaving the Hubble radius at that point. While ϕ evolves, quantum fluctuations imprint scalar and gravity-wave perturbations upon each scale as it leaves the Hubble radius. The scalar perturbations depend upon the potential and its derivative, while the gravitational modes depend only upon the potential. In principle, A_G and A_S are probed by observations of large-scale structure and by measurements of CMBR fluctuations. The length scale, and corresponding angular scales, of several important observations are indicated.

In the next section we will discuss the procedure for reversing the process discussed in this section; knowing $A_G(\lambda)$ and $A_S(\lambda)$, how does one determine $V(\phi)$?

III. RECONSTRUCTION OF THE POTENTIAL

A number of authors [12,18,19,20] have recently emphasized the possibility that tensor modes excited during inflation, corresponding to gravitational waves, may play an important role in generating microwave background anisotropies. We thus develop an extension of the potential reconstruction methods of Hodges and Blumenthal [7] to include tensor as well as scalar modes. As discussed in the previous section, the expressions for the amplitudes of the scalar and tensor modes may be written as

$$\begin{aligned} A_S(\phi) &= \frac{\sqrt{2}\kappa^2}{8\pi^{3/2}} \frac{H^2(\phi)}{|H'(\phi)|} \\ A_G(\phi) &= \frac{\kappa}{4\pi^{3/2}} H(\phi), \end{aligned} \tag{3.1}$$

respectively. Note that the definition of $A_S(\phi)$ in Eq. (3.1) is related to the power spectrum $P^{1/2}(k)$ defined in Hodges and Blumenthal [7] by

$$P^{1/2}(k) = 3\sqrt{2\pi} A_S(\phi). \tag{3.2}$$

Utilizing the slow-roll approximation, there are useful expressions for the scale-dependence of the spectra, the *spectral indices*, to first-order in departure from slow-roll. These are

$$\begin{aligned} 1 - n \equiv & \; d\ln[A_S^2(\lambda)]/d\ln\lambda &= 4\epsilon_* - 2\eta_* \\ n_G \equiv & \; d\ln[A_G^2(\lambda)]/d\ln\lambda &= 2\epsilon_* \end{aligned} \tag{3.3}$$

where "$*$" indicates evaluation at the time when the scale λ passes outside the Hubble radius during inflation. In keeping with convention we drop the subscript S on the scalar mode index. Whenever the slow-roll conditions are closely obeyed, the spectrum is close to scale invariant. When this is not true, there are in general corrections to the expressions for the fluctuations at the next order in an expansion in slow-roll parameters.

The reader may have noticed that although we are keeping the equations of motion general (*i.e.*, not subject to a slow-roll approximation), our expression for the scalar modes in Eq. (3.1) is an expression based on the slow-roll approximation, $\{\epsilon, |\eta|\} \ll 1$. Ideally, one would like to completely abandon the slow-roll regime, because within it, the scalar spectrum is always close to the scale-invariant case and the gravitational wave amplitude is always small, as we have seen. In practice, it seems very possible that should inflation have occurred, it may well have been pushing the outside of the slow-roll approximation envelope, and indeed much of the recent interest has been in the possibilities of both tilt and gravitational waves. True reconstruction assumes nothing about $V(\phi)$ (flatness, etc.) except that it inflates. Unfortunately, although we are able to keep the dynamics completely general, general expressions are not available for the perturbation spectra.

Recently, an improvement has become available in the form of general expressions for the spectra to first-order in departure from slow-roll [21]. These give rise to "first-order corrected" spectra, which can be written

$$\begin{aligned} A_S^{\rm corr} &= [1-\epsilon+(2-\ln 2-\gamma)(2\epsilon-\eta)]A_S^{\rm uncorr} \\ A_G^{\rm corr} &= [1+(1-\ln 2-\gamma)\epsilon]A_G^{\rm uncorr}, \end{aligned} \tag{3.4}$$

where $\gamma \simeq 0.577$ is Euler's constant. If slow-roll is breaking then these can represent a significant improvement on the uncorrected results, but unfortunately the reconstruction loses its analytic tractability. The one exception to this is the case of power-law inflation —in that case the effects of the corrections cancel exactly [22] in the reconstruction equation Eq. (3.10) we derive below.

Rather than resort immediately to numerical construction, we elect instead to make the operational choice that we shall adopt the slow-roll expressions for the spectra. A reconstruction can then be made subject to a consistency check that the slow-roll conditions are indeed satisfied; if not, then our formalism will have to be enhanced to incorporate these improvements.

It is clear that the ratio of amplitudes of the scalar and tensor modes is given by

$$\frac{A_G}{A_S} = \frac{\sqrt{2}}{\kappa}\frac{|H'|}{H} = \sqrt{\epsilon}, \tag{3.5}$$

and if $\epsilon \ll 1$, then $A_G/A_S \ll 1$. It is possible that the *COBE* satellite is in fact observing a sum of contributions from the tensor and scalar fluctuations, as opposed to the pure scalar modes as originally thought. If these are uncorrelated and obey Gaussian statistics, the quantity of observational interest on large angular scales is the sum of the squares[7]

$$S^2(\phi) = \frac{m^2}{2}A_S^2(\phi) + A_G^2(\phi). \tag{3.6}$$

Using $m = 2/5$ and recalling that ϵ must be less than unity, we see immediately that the tensor modes dominate $S^2(\phi)$ if $2/25 < \epsilon < 1$, or equivalently if $\kappa/5 < |H'|/H < \kappa/\sqrt{2}$. The largest relative tensor contribution to $S^2(\phi)$ obtains for $\epsilon = 1$: $2A_G^2/m^2A_S^2 = 25/2$ for $m = 2/5$.[8] Although it is not mandatory (one can break slow-roll only in the η parameter as in natural inflation), the gravitational wave contribution is typically significant whenever there is a deviation from the slow-roll regime.

On the other hand, the gravitational waves behave as relativistic matter when they re-enter the Hubble radius and do not interact with the other matter components.

[7]The relative weighting of A_S^2 and A_G^2 in this equation is that appropriate to large angle anisotropies (greater than 2°) in the slow-roll approximation. This is discussed in depth in Section VI, and exact weighting formulae provided there.

[8]If one is performing a theoretical reconstruction of the potential by specifying either A_G or A_S, it is essential to ensure this condition is always satisfied for consistency. Indeed, observations violating $A_G/A_S < 1$ would immediately rule out the models we are considering.

Consequently their energy density redshifts as a^{-4}, which implies that only scalar modes affect the CMBR anisotropy on angular scales $\theta \ll 2°$. However the anisotropy on these scales is also affected by the form of dark matter present. [For a recent discussion of some of these issues, see Ref. (23).]

To proceed, we shall assume that the functional forms of $A_S(\lambda)$ and $A_G(\lambda)$ are known explicitly and defer until Section VI a discussion on the many difficulties associated with determining these quantities from observation. Our initial aim is to develop a framework which allows the inflaton potential to be determined. We consider general inflationary behavior for the field equations (2.9) and (2.10) and it proves convenient to parameterize the full set of solutions in terms of the function $H(\lambda(\phi))$, where λ is the scale. Eqs. (3.1) now become

$$\begin{aligned} A_S(\lambda) &= \frac{\sqrt{2}\kappa^2}{8\pi^{3/2}} H^2(\lambda) \left| \frac{d\lambda}{dH} \frac{d\phi}{d\lambda} \right| \\ A_G(\lambda) &= \frac{\kappa}{4\pi^{3/2}} H(\lambda). \end{aligned} \tag{3.7}$$

Each length scale λ is associated with a unique value of ϕ when that scale crossed the Hubble radius during inflation. We will indicate that relationship by writing $\lambda(\phi)$. Now when a present length scale λ crossed the Horizon radius during inflation with scalar field value ϕ, its physical size was $H^{-1}(\phi)$. The physical size grew between horizon crossing and today, and is now simply $\lambda(\phi) = H^{-1}(\phi)a_0/a(\phi)$, where a_0 is the present value of the scale factor and $a(\phi)$ was the value of the scale factor when the scale crossed the Hubble radius during inflation. Now we can make use of Eq. (2.17) to relate $a(\phi)$ to the value of the scale factor at the end of inflation, a_e: $a(\phi) = a_e \exp[-N(\phi)]$. This allows us to express $\lambda(\phi)$ as

$$\lambda(\phi) = \frac{\exp[N(\phi)]}{H(\phi)} \frac{a_0}{a_e}, \tag{3.8}$$

where $N(\phi)$ is given by Eq. (2.17). Differentiating Eq. (3.8) with respect to ϕ yields

$$\frac{d\lambda(\phi)}{d\phi} = \pm \frac{\kappa}{\sqrt{2}} \left(\frac{A_S}{A_G} - \frac{A_G}{A_S} \right) \lambda, \tag{3.9}$$

and taking the ratio of Eqs. (3.7) implies[9]

$$\frac{\kappa}{\sqrt{2}} \frac{A_G}{A_S} = \left| \frac{d\lambda}{d\phi} \frac{d \ln A_G}{d\lambda} \right|. \tag{3.10}$$

Note that expression (2.10) in Hodges and Blumenthal [7] consists of only our first term in Eq. (3.9), indicating their assumption of slow-roll behavior. Substituting Eq. (3.9) into Eq. (3.10) gives

$$\frac{\lambda}{A_G(\lambda)} \frac{dA_G(\lambda)}{d\lambda} = \frac{A_G^2(\lambda)}{A_S^2(\lambda) - A_G^2(\lambda)}. \tag{3.11}$$

[9] If one were to use the 'first-order corrected' expressions for the spectra discussed earlier, the right hand side of Eq. (3.10) would be multiplied by $(1 - 1.27\epsilon + 1.27\eta)$.

Note that the left hand side is just equal to $n_G/2$. This equation is similar to Eq. (9) in Davis *et al.* [19], provided one interprets their n as being the tensor index and not the scalar one. It clearly shows that there exists a correspondence between the scalar and tensor modes and is valid for an arbitrary interaction potential. In principle, if the scale dependence of either the scalar *or* tensor modes is known, the other can be determined from Eq. (3.11). If only $A_G(\lambda)$ is known, then $A_S(\lambda)$ follows immediately by differentiation. However, if only $A_S(\lambda)$ is known, a first-order differential equation must be solved to find the form of $A_G(\lambda)$. Thus, knowledge of only the scalar spectrum leaves an undetermined constant in the tensor spectrum.

Once the form of the tensor spectrum is known, the potential, as parametrized by λ, may be derived by substituting Eqs. (3.7) into Eq. (3.10). We find

$$V[\phi(\lambda)] = \frac{16\pi^3 A_G^2(\lambda)}{\kappa^4}\left[3 - \frac{A_G^2(\lambda)}{A_S^2(\lambda)}\right]. \tag{3.12}$$

Finally, integration of Eq. (3.9) yields the function $\phi = \phi(\lambda)$ given by

$$\phi(\lambda) = \pm\frac{\sqrt{2}}{\kappa}\int^{\lambda} \frac{d\lambda'}{\lambda'}\frac{A_S(\lambda')A_G(\lambda')}{A_S^2(\lambda') - A_G^2(\lambda')}. \tag{3.13}$$

We have absorbed the integration constant by taking advantage of the freedom to shift ϕ by a constant. The functional form of $V(\phi)$ follows by inverting Eq. (3.13) and substituting the result into Eq. (3.12). It will also prove convenient at times to express ϕ in terms of A_G. If the functional form of A_S as a function of A_G is known, $A_S[A_G]$, then using Eq. (3.11) in Eq. (3.13) gives

$$\phi = \pm\frac{\sqrt{2}}{\kappa}\int^{A_G} dA'_G \frac{A_S[A'_G]}{A'^2_G}. \tag{3.14}$$

The reconstruction equations are Eqs. (3.11), (3.12), and (3.13). It is worth emphasizing again that for any choice of $A_G(\lambda)$, there is a unique associated $A_S(\lambda)$ and $V(\phi)$ (at least in the slow-roll approximation), but that the converse is not true. As shown by Hodges and Blumenthal [7], the scalar spectrum leaves an undetermined constant in the tensor spectrum, and as the equation relating V and A_G is non-linear, different choices of this constant might lead to functionally different forms of the potential [24]. In order to reconstruct the potential from scalar modes, one needs an additional piece of information. Technically what is needed is knowledge of the functional dependence of A_S upon A_G, $A_S[A_G]$. This can be fixed either by knowledge of the amplitude of the tensor spectrum at a single scale, which would fix A_G uniquely, or knowledge that A_S is independent of A_G. As A_G cannot be independent of λ, the latter possibility arises only if $A_S(\lambda)$ is constant.

It is also worth emphasising consistency, which can provide an important check. If our inflationary assumptions are correct, then the two spectra are intimately related as illustrated above. However, observations are typically subject to both systematic and statistical errors, and within these one might find that measured spectra are not

exactly consistent. Were one to be confronted with such data, one would like some prescription by which to decide how to best reconcile the data, to generate some kind of "maximum likelihood" reconstruction. Such a procedure would presumably also allow one to demonstrate that the measured spectra were not compatible with each other within the inflationary paradigm, if indeed inflation were not the correct source of the fluctuations. In practice, the situation is skewed by the scalar fluctuations being considerably easier to observe than their tensor counterparts, and it seems prudent to await the arrival of considerably better data before properly contemplating how one would deal with the possibility of marginally incompatible observations.

The reconstruction procedure simplifies if $A_G(\lambda) \ll A_S(\lambda)$ (i.e., $\epsilon \ll 1$):

$$\begin{aligned} \frac{\lambda}{A_G(\lambda)}\frac{dA_G(\lambda)}{d\lambda} &= \frac{A_G^2(\lambda)}{A_S^2(\lambda)} \\ \phi(\lambda) &= \pm\frac{\sqrt{2}}{\kappa}\int^{\lambda}\frac{d\lambda'}{\lambda'}\frac{A_G(\lambda')}{A_S(\lambda')} \\ V[\phi(\lambda)] &= \frac{48\pi^3}{\kappa^4}A_G^2(\lambda). \end{aligned} \tag{3.15}$$

We conclude this section by summarizing the conditions necessary for the perturbation amplitudes to increase or decrease with increasing wavelength. Such information alone can place strong limits on the functional form of the potential. The scales that first cross the Hubble radius are the last to re-enter during the radiation or matter dominated eras (see Fig. 1). Consequently, the amplitudes of the modes increase (decrease) with wavelength if they decrease (increase) with time during inflation. Immediately we conclude that

$$\frac{dA_G}{d\lambda} > 0 \tag{3.16}$$

for all sub-inflationary ($\dot{H} < 0$) models. One requires an era of super-inflation ($\dot{H} > 0$) if this inequality is to be reversed. Super-inflation is only possible with a minimally coupled self-interacting scalar field if the spatial hypersurfaces of the manifold have positive-definite curvature [9]. An observation indicating $dA_G/d\lambda < 0$ would therefore require some of the main assumptions made in the inflationary analysis to be significantly altered. Within the context of the FRW Universe, for example, one would need to extend the gravitational sector of the theory beyond general relativity, or assume that the value of the density parameter was significantly larger than unity at first Hubble radius crossing. Indeed, Eq. (3.16) implies that any effects of the gravitational waves on the CMBR anisotropy will always be enhanced on larger angular scales in the models considered here.

On the other hand, it is possible for the scalar spectrum to decrease with wavelength. By writing $dA_S/d\lambda = (dA_S/d\phi)(d\phi/d\lambda)$ and employing Eqs. (3.7) and (3.9), one finds that a necessary and sufficient condition for scalar modes to be decreasing

in amplitude with increasing wavelength is

$$\left(\frac{H'}{H}\right)^2 < \frac{1}{2}\frac{H''}{H}. \tag{3.17}$$

In terms of the slow-roll parameters, this can be written as $2\epsilon < \eta$. As ϵ is positive by definition, this condition is not easy to satisfy, particularly in the late stages of inflation where ϵ must increase towards unity. A necessary, but not sufficient, condition for Eq. (3.17) to hold is that the potential be *convex*, $V'' > 0$. Therefore, if the field is located near a local maximum of the potential, as in natural inflation [25] for example, the amplitude will always increase with λ.

In conclusion, it is clear that any scale dependence for the spectrum of gravitational waves is possible in principle, subject to condition (3.16). Secondly, the most useful parameter *mathematically* in the reconstruction process is $A_G(\lambda)$, because once this is known the potential can be derived in a rather straightforward manner.

IV. RECONSTRUCTING THE FULL POTENTIAL

Before proceeding to analyze the possibilities for obtaining the spectra observationally, we shall first illustrate some examples in reconstruction in order to demonstrate the techniques. We shall examine four cases of increasing complexity. These four cases will reconstruct to familiar potentials.

A. Polynomial potentials

Let us first reconstruct the $\mu^2\phi^2$ chaotic potential model worked out in Section II. We will then generalize the result for construction of polynomial potentials.

Recall that using the slow-roll approximation for the potential $V(\phi) = \mu^2\phi^2$ we found perturbation spectra $A_G(\lambda) = \alpha[\beta + \ln(\lambda/\lambda_0)]^{1/2}$ and $A_S(\lambda) = \sqrt{2}A_G^2(\lambda)/\alpha$, with $\alpha^2 = \kappa^2\mu^2/12\pi^3$, $\beta = 45.5$, and $\lambda_0 = 1$ Mpc. We must keep in mind that these solutions were obtained in the slow-roll approximation. Since the slow-roll approximation implies that $A_G \ll A_S$, we must reconstruct using Eqs. (3.15).

First, let us reconstruct assuming that observations provide two pieces of information: $A_G(\lambda)$ is of the form $A_G(\lambda) = \alpha[\beta + \ln(\lambda/\lambda_0)]^{1/2}$, and $A_G(\lambda) \ll A_S(\lambda)$. Then the differential equation for $dA_G(\lambda)/d\lambda$ in Eq. (3.15) can be used to yield a unique scalar spectrum, $A_S(\lambda) = \sqrt{2}A_G^2(\lambda)/\alpha$, as anticipated from the calculation in Section II. (Of course $A_S(\lambda)$ could be found without the assumption that $A_G(\lambda) \ll A_S(\lambda)$, but it would be different.)

Now that we know both $A_G(\lambda)$ and $A_S(\lambda)$, we can find $\phi(\lambda)$ from the second

equation in Eq. (3.15):

$$\beta + \ln(\lambda/\lambda_0) = \kappa^2\phi^2/4. \tag{4.1}$$

Finally, we can use the last equation in the slow-roll reconstruction procedure to give

$$V(\phi) = \frac{48\pi^3}{\kappa^4}A_G^2(\lambda) = \frac{48\pi^3}{\kappa^4}\alpha^2[\beta + \ln(\lambda/\lambda_0)] = \frac{12\pi^3}{\kappa^2}\alpha^2\phi^2. \tag{4.2}$$

Exactly as expected, the potential is of the form $V(\phi) = \mu^2\phi^2$, with $\mu^2 = 12\pi^3\alpha^2/\kappa^2$. Thus, we have successfully reconstructed the potential.

We began with the assumption that $A_G(\lambda)$ is known. If we had started with the assumption that the scalar spectrum is known and of the form $A_S(\lambda) = \sqrt{2}\alpha[\beta + \ln(\lambda/\lambda_0)]$, the differential equation for $A_G(\lambda)$ would give

$$A_G^{-2}(\lambda) = \alpha^{-2}[\beta + \ln(\lambda/\lambda_0)]^{-1} + C, \tag{4.3}$$

where C is arbitrary. Fixing $A_G(\lambda_0) = \alpha\beta^{1/2}$ fixes $C = 0$, and reconstruction would proceed exactly as before. Other choices of C would lead to different potentials, with different predictions for A_G.

Now let's consider a slightly more general tensor mode spectrum: $A_G = \alpha[\beta + \ln(\lambda/\lambda_0)]^\gamma$ with $\gamma =$ constant, again with $A_G(\lambda) \ll A_S(\lambda)$. The differential equation for $dA_G(\lambda)/d\lambda$ gives

$$A_S(\lambda) = [\alpha/\sqrt{\gamma}]\,[\beta + \ln(\lambda/\lambda_0)]^{(2\gamma+1)/2}. \tag{4.4}$$

The solution for $\phi(\lambda)$ is the same as Eq. (4.1) with $\kappa \to \kappa/\sqrt{2\gamma}$. Using this in the reconstruction of the potential gives

$$V(\phi) = \frac{48\pi^3}{\kappa^4}A_G^2(\lambda) = \frac{48\pi^3}{\kappa^{4(1-\gamma)}}\frac{\alpha^2}{(8\gamma)^{2\gamma}}\phi^{4\gamma}. \tag{4.5}$$

An oft studied case is $\gamma = 1$, which reconstructs to $V(\phi) = \lambda\phi^4$ with scalar and tensor perturbations

$$\begin{aligned} A_G(\lambda) &= \alpha\,[\beta + \ln(\lambda/\lambda_0)] \\ A_S(\lambda) &= \alpha\,[\beta + \ln(\lambda/\lambda_0)]^{3/2}. \end{aligned} \tag{4.6}$$

B. Harrison–Zel'dovich potentials

Let us now look at potentials which give rise to the Harrison–Zel'dovich spectrum, $A_S(\lambda) = a_S =$ constant. Such spectra are actually rather unlikely; most inflationary models exhibit a decrease in amplitude with decreasing scale which is significant now given the accuracy of observations.

We start reconstruction by considering the differential equation relating A_G and A_S [Eq. (3.11)]:

$$\frac{\lambda}{A_G(\lambda)}\frac{dA_G(\lambda)}{d\lambda} = \frac{A_G^2(\lambda)}{a_S^2 - A_G^2(\lambda)}, \tag{4.7}$$

which has solution

$$\ln(\lambda/\lambda_0) = -\frac{a_S^2}{2}\left(\frac{1}{A_G^2(\lambda)} - \frac{1}{A_{G0}^2}\right) - \ln(A_G(\lambda)/A_{G0}). \tag{4.8}$$

In general there is no closed-form expression for $A_G(\lambda)$.

We can reconstruct the potential in two steps. Since A_S is a constant, we can find A_G in terms of ϕ by Eq. (3.14):

$$A_G^2(\phi) = 2a_S^2/\kappa^2\phi^2. \tag{4.9}$$

Now we can substitute this into the equation for V in Eq. (3.12) to give

$$V(\phi) = \frac{16\pi^3}{\kappa^4}a_S^2\left[3\frac{1}{(\phi/\bar{\phi})^2} - \frac{1}{(\phi/\bar{\phi})^4}\right] \tag{4.10}$$

where $\bar{\phi} = \sqrt{2}/\kappa$.

It should be emphasized that this is the *only* inflaton potential which leads to an *exactly* scale-invariant spectrum of scalar density fluctuations. It arises as a special case of "intermediate" inflation [26], where the scale factor expands as $a \propto \exp(t^f)$ with $0 < f < 1$; the above potential corresponds to choosing $f = 2/3$. In contrast, the spectrum of gravitational waves is not scale invariant. It is generally true that inflation cannot lead to scalar and tensor perturbation spectra that are *both* constant in λ. It is interesting to note that potentials of this form arise when supersymmetry is spontaneously broken [27].

We can reinterpret these results in terms of the slow-roll parameters. It is clear that to obtain a flat spectrum we require $2\epsilon = \eta$, but ϵ and η are not determined separately. There are some interesting limiting cases. If we allow a_S to tend to infinity, this corresponds to ϵ tending to zero. In this limit the potential becomes flat, with its constant value being that which gives the desired gravitational wave amplitude. As a_S is reduced from infinity, ϵ increases away from zero preserving $2\epsilon = \eta$. Once ϵ becomes big enough, there will be slow-roll corrections which destroy the flatness of the spectrum. It is interesting to note that although slow-roll automatically guarantees a spectrum which is close to flat, it is perfectly possible for a spectrum close to flatness to arise when the slow-roll conditions are not well obeyed.

These potentials, which exhibit little tilt but which can have substantial gravitational waves, are also of interest in that they complete a square of possible behaviors in different inflationary models, as shown in Table 1. Indeed, such a model performs well on most large-scale structure data with the exception of intermediate-scale galaxy clustering data.

Scalar Spectrum	Small gravitational wave contribution	Large gravitational wave contribution
Nearly flat spectrum	Polynomial potentials	Harrison-Zel'dovich potential
Tilted spectrum	Hyperbolic potentials	Exponential potentials

Table 1: Possible behaviors for spectra in several inflationary models.

C. Exponential potentials

Generalizing away from the flat scalar spectrum, the simplest (and possibly most likely) case is where the amplitudes have a simple power-law dependence,

$$A_S(\lambda) = a_S(\lambda/\lambda_0)^\nu, \qquad \nu \neq 0, \tag{4.11}$$

where a_S is a constant. The recent measurements from *COBE* [1] alone provide the constraint $-0.3 < \nu < 0.2$ at the 1-sigma level. Incorporating specific choices of dark matter and including clustering data allows one to do better; for instance in a cold dark matter model (CDM) it has been shown [28] that $\nu < 0.15$ at 95% confidence in models with no gravitational waves, and $\nu < 0.08$ (again 95% confidence) in power-law inflation which does have significant gravitational wave production.

$A_G(\lambda)$ satisfies the differential equation Eq. (3.11)

$$\frac{\lambda}{A_G(\lambda)}\frac{dA_G(\lambda)}{d\lambda} = \frac{A_G^2(\lambda)}{a_S^2(\lambda/\lambda_0)^{2\nu} - A_G^2(\lambda)}. \tag{4.12}$$

Obtaining the general form for $A_G(\lambda)$ is difficult. However there are some specific solutions which are of interest in that they relate to known examples of inflationary potentials. One obvious solution to Eq. (4.12) is $A_G(\lambda) = a_g(\lambda/\lambda_0)^\nu$, with

$$a_g^2 = \left(\frac{\nu}{1+\nu}\right) a_S^2, \qquad \nu \neq 0. \tag{4.13}$$

Note that in this simple case, $A_G/A_S = a_g/a_S$, a constant independent of scale, but that as $\nu \to 0$ the magnitude of the tensor contribution reduces significantly. We can simply integrate Eq. (3.13) to obtain

$$\phi(\lambda) = \pm\sqrt{\frac{2}{\kappa^2}}\ln\left(\frac{\lambda}{\lambda_0}\right)\sqrt{\nu^2+\nu}. \tag{4.14}$$

Substituting this expression into Eq. (3.12) gives the final result

$$V(\phi) = V_0 \exp(\pm\phi/\bar{\varphi}), \tag{4.15}$$

with

$$V_0 = \frac{16\pi^3 a_g^2}{\kappa^4}\frac{2\nu+3}{\nu+1}; \qquad \bar{\phi}^{-1} = \kappa\sqrt{\frac{2\nu}{\nu+1}}. \tag{4.16}$$

Thus we see that a power-law behavior for the amplitude of the scalar and tensor modes is obtained from an exponential potential, and is therefore consistent with power-law models of inflation [10].

It is interesting to note that this result for $\bar{\phi}$ coincides with the exact result for power-law inflation, whereas if slow-roll were strictly applied one would get $\bar{\phi}^{-1} = \kappa\sqrt{2\nu}$, being the above to lowest order in ν. Thus our hybrid of general equations of motion but slow-roll spectrum definitions certainly offers improved results over the usual slow-roll method in this case.

Note that as $\nu \to +\infty$ the relative slope of the potential, as determined by α, becomes independent of ν. The limit $\alpha(\nu = \infty) = \sqrt{2}\kappa$ corresponds to the Milne Universe $a(t) \propto t$ and represents the limiting solution for inflation to occur. As ν is increased in Eq. (4.15) the only real effect is to increase the height of the potential through the V_0 term.

Rather than the equal power behavior, consider the more general example

$$A_S(\lambda) = a_S(\lambda/\lambda_0)^\nu\ ; \qquad A_G(\lambda) = a_G(\lambda/\lambda_0)^\sigma, \tag{4.17}$$

where a_S and a_G are constants. It is trivial to show that these spectra are solutions to Eq. (3.11) or the differential equation in Eq. (3.15) *only* if $\sigma = \nu$. Thus, observation of spectra that are exact power-laws with different powers would rule out the class of inflationary models we consider as the source of the perturbations.

D. Hyperbolic potentials

Let us return to the differential equation for $A_G(\lambda)$ in Eq. (4.12), but in the $A_G(\lambda) \ll A_S(\lambda)$ limit. The equation becomes

$$\frac{dA_G}{d\lambda} = \frac{A_G^3}{\lambda}\frac{1}{a_S^2}(\lambda/\lambda_0)^{-2\nu}. \tag{4.18}$$

This equation has general solution in terms of an undetermined constant β:

$$A_G^2(\lambda) = a_S^2\nu\frac{(\lambda/\lambda_0)^{2\nu}}{1+\beta(\lambda/\lambda_0)^{2\nu}}. \tag{4.19}$$

We will see that different functional forms for the potential reconstruct depending upon the sign of β. Of course β can be determined by measurement of A_G on any one scale.

As $\beta \to 0$ we recover the power-law spectra for $A_G(\lambda)$ and $A_S(\lambda)$ with equal power-law slopes. This case was just considered above. For small scales, $|\beta|\,(\lambda/\lambda_0)^{2\nu} \ll 1$,

we also recover the above case of equal power-law slopes for either choice of the sign of β. For $\beta > 0$ we can take the limit of large scales, $\beta(\lambda/\lambda_0)^{2\nu} \gg 1$, in which case $A_G(\lambda)$ asymptotically approaches a constant.

Recall that in the $A_G \ll A_S$ reconstruction procedure, Eq. (3.15) gives

$$V[\phi(\lambda)] = \frac{48\pi^3}{\kappa^4} A_G^2(\lambda). \tag{4.20}$$

Now we must find $\phi(\lambda)$ and invert.

The integral expression for $\phi(\lambda)$ from Eq. (3.15) is

$$\phi/\bar{\phi} = 2\nu \int^{\lambda} \frac{d\lambda'}{\lambda'} \frac{1}{[1 \pm |\beta|(\lambda'/\lambda_0)^{2\nu}]^{1/2}}, \tag{4.21}$$

with "+" for positive β and "−" for negative β. The constant $\bar{\phi}$ is the same as that of the previous subsection (in the slow-roll approximation), $\bar{\phi}^{-1} = \kappa\sqrt{2\nu}$. The solutions to the integral are

$$\phi/\bar{\phi} = \begin{cases} -2\mathrm{Arccsch}\left[\sqrt{\beta}\,(\lambda/\lambda_0)^{\nu}\right] & \beta > 0 \\ \\ -2\mathrm{Arcsech}\left[\sqrt{|\beta|}\,(\lambda/\lambda_0)^{\nu}\right] & \beta < 0. \end{cases} \tag{4.22}$$

These expressions are easily inverted to give $\lambda(\phi)$, and the potential reconstructs to

$$V(\phi) = V_0 \begin{cases} \cosh^{-2}(\phi/2\bar{\phi}) & \beta > 0 \\ \\ \sinh^{-2}(\phi/2\bar{\phi}) & \beta < 0, \end{cases} \tag{4.23}$$

with $V_0 = 48\pi^3 a_S^2 \nu/\kappa^4|\beta|$.

Note that for $\phi/\bar{\phi} \gg 1$, $V(\phi) \propto \exp(-\phi/\bar{\phi})$ for both choices of the sign of β. Large values of ϕ cross the Hubble radius late in inflation and correspond to small λ. Notice from Eq. (4.19) that $A_G \to \lambda^{\nu}$ as $\lambda \to 0$. We have already reconstructed the potential that results from this $A_G(\lambda)$ as $V(\phi/\bar{\phi}) \propto \exp(-\phi/\bar{\phi})$, which agrees with the definition of $\bar{\phi}$ given in Eq. (4.16) when $\nu \ll 1$. (The assumption that $A_G \ll A_S$ is equivalent to this condition).

We can also expand Eq. (4.23) for small ϕ:

$$V(\phi) \longrightarrow V_0 \begin{cases} 1 - (\phi/\bar{\phi})^2/4 + \cdots & \beta > 0 \\ \\ 4(\phi/\bar{\phi})^{-2} + \cdots & \beta < 0. \end{cases} \tag{4.24}$$

The positive β case is also an approximation to a potential of the form $V(\phi) \propto 1 + \cos(\phi/\bar{\phi})$ as studied in a type of model called natural inflation [25].

The purpose of the above reconstruction exercises is to demonstrate how the reconstruction process proceeds. We have reconstructed several popular inflationary potentials from knowledge of either the scalar or tensor perturbation spectrum. Before

turning to the prospectus for actually determining A_S and A_G from observational data, in the next section we discuss a "perturbative" approach in reconstruction of the potential.

V. RECONSTRUCTING A PIECE OF THE POTENTIAL

The reconstruction program described in the previous section is quite ambitious, as it depends upon knowledge of the functional forms of $A_G(\lambda)$ and/or $A_S(\lambda)$ over a range of λ. In this section we will outline a less ambitious, but more realistic program. We will assume that we have information only about the scalar and tensor spectra (and their first and second derivatives) at a single scale λ_0, and see what we can learn about the potential.[10] This "perturbative" approach to reconstruction may be useful in the very near future [23].

If we know $A_G(\lambda_0)$ and $A_S(\lambda_0)$ at some length scale λ_0 (which left the Hubble radius during inflation when the value of the scalar field was ϕ_0), we can use Eqs. (3.9) and (3.13) to find that

$$\begin{aligned} \frac{1}{\lambda}\frac{d\lambda}{d\phi}\bigg|_{\lambda=\lambda_0} &= \pm\frac{\kappa}{\sqrt{2}}\frac{A_S^2(\lambda_0)-A_G^2(\lambda_0)}{A_S(\lambda_0)A_G(\lambda_0)}, \\ \frac{dA_G(\lambda)}{d\lambda}\bigg|_{\lambda=\lambda_0} &= \frac{1}{\lambda_0}\frac{A_G^3(\lambda_0)}{A_S^2(\lambda_0)-A_G^2(\lambda_0)}. \end{aligned} \tag{5.1}$$

$V(\phi_0)$ immediately follows from $A_G(\lambda_0)$ and $A_S(\lambda_0)$:

$$V(\phi_0) = \frac{16\pi^3}{\kappa^4}\left[3A_G^2(\lambda_0) - \frac{A_G^4(\lambda_0)}{A_S^2(\lambda_0)}\right]. \tag{5.2}$$

With the approximation that $A_G(\lambda_0) \ll A_S(\lambda_0)$, the expression simplifies to

$$V(\phi_0) = \frac{48\pi^3}{\kappa^4}A_G^2(\lambda_0)\left[1+\mathcal{O}\left(\frac{A_G^2(\lambda_0)}{A_S^2(\lambda_0)}\right)\right]. \tag{5.3}$$

Further reconstruction of the potential requires more than simply knowledge of the amplitudes of the scalar and tensor perturbations at λ_0, we must know the first derivative, or the spectral index of the scalar spectrum at $\lambda = \lambda_0$:

$$\frac{1}{A_S(\lambda)}\frac{dA_S(\lambda)}{d\lambda}\bigg|_{\lambda=\lambda_0} = \frac{1-n}{2\lambda}\bigg|_{\lambda=\lambda_0} = \frac{1-n_0}{2\lambda_0}. \tag{5.4}$$

[10] In practice, observing the derivatives at a single point may be just as difficult as measuring the shape over a range of scales, though one might hope for adequate information to be obtained from a significantly smaller range of scales (and with more freedom to coarse-grain), perhaps even those accessible from a single experiment.

Using Eqs. (5.1) and (5.2) we can find the first derivative of the potential:

$$V'(\phi_0) \equiv \left.\frac{dV(\phi)}{d\phi}\right|_{\lambda=\lambda_0} = \pm\frac{16\pi^3}{\sqrt{2}\kappa^3}\frac{A_G^3(\lambda_0)}{A_S(\lambda_0)}\left[7 - n_0 - (5-n_0)\frac{A_G^2(\lambda_0)}{A_S^2(\lambda_0)}\right]. \tag{5.5}$$

This expression also simplifies in the $A_G(\lambda_0) \ll A_S(\lambda_0)$ limit:

$$V'(\phi_0) = \pm\frac{16\pi^3}{\sqrt{2}\kappa^3}\frac{A_G^3(\lambda_0)}{A_S(\lambda_0)}(7-n_0)\left[1 + \mathcal{O}\left(\frac{A_G^2(\lambda_0)}{A_S^2(\lambda_0)}\right)\right]. \tag{5.6}$$

Repeated differentiation of this expression with respect to ϕ enables one to derive the higher derivatives. In principle, the potential can then be expanded as a Taylor series about the point ϕ_0. The full expression for the second derivative is

$$\begin{aligned} V''(\phi_0) \;=\; & \frac{8\pi^3}{\kappa^2}\frac{A_G^2(\lambda_0)}{A_S^2(\lambda_0)}\left\{3A_G^2(\lambda_0)\left[7 - n_0 - (5-n_0)\frac{A_G^2(\lambda_0)}{A_S^2(\lambda_0)}\right]\right. \\ & -\left(\frac{1-n_0}{2}\right)\left[7 - n_0 - (5-n_0)\frac{A_G^2(\lambda_0)}{A_S^2(\lambda_0)}\right]\left[A_S^2(\lambda_0) - A_G^2(\lambda_0)\right] \\ & +\left[A_S^2(\lambda_0) - A_G^2(\lambda_0)\right]\left[\left(-1 + \frac{A_G^2(\lambda_0)}{A_S^2(\lambda_0)}\right)\lambda_0 n_0'\right. \\ & -2(5-n_0)\frac{A_G^4(\lambda_0)}{A_S^2(\lambda_0)}\frac{1}{A_S^2(\lambda_0) - A_G^2(\lambda_0)} \\ & \left.\left.+(5-n_0)(1-n_0)\frac{A_G^2(\lambda_0)}{A_S^2(\lambda_0)}\right]\right\}, \end{aligned} \tag{5.7}$$

where $n_0' \equiv dn_0/d\lambda_0$. If one makes the approximation that $A_G(\lambda_0) \ll A_S(\lambda_0)$, it follows that this expression simplifies considerably:

$$\begin{aligned} V''(\phi_0) \;=\; & \frac{4\pi^3}{\kappa^2}\frac{A_G^2(\lambda_0)}{A_S^2(\lambda_0)}\left[4(n_0-4)^2A_G^2(\lambda_0) - (1-n_0)(7-n_0)A_S^2(\lambda_0)\right] \\ & \times\left\{1 + \mathcal{O}\left(\frac{A_G^2(\lambda_0)}{A_S^2(\lambda_0)}\right) + \mathcal{O}\left(\left.\frac{dn_0}{d\ln\lambda}\right|_{\lambda=\lambda_0}\right)\right\}. \end{aligned} \tag{5.8}$$

Note that $(1-n_0)$ is in principle of the same order as A_G^2/A_S^2.

It is hoped that observations will soon be of a sufficient standard to measure $A_G(\lambda_0)$, $A_S(\lambda_0)$ and n_0 at a particular point. One may then be able to establish whether the potential is convex or concave with the use of Eq. (5.8). The potential is convex in any model where the scalar spectrum decreases with increasing wavelength. Note though that this is only sufficient, not necessary. Indeed, most popular models such as polynomial and exponential potentials are convex yet still feature a spectrum increasing with increasing wavelength. In models where the tensor contribution is negligible, the only important parameter is the sign of $1-n_0$, since $n_0 > 7$ is already ruled out by observation

Another quantity of interest that may soon be determined observationally is the dimensionful parameter $V(\phi_0)/|V'(\phi_0)|$. This is determined by the relative amplitudes of the scalar and tensor fluctuations at a given scale via Eq. (3.5). In this sense, such a quantity yields information regarding a mass scale at which these processes are occurring during inflation. In the case of polynomial potentials it uniquely determines ϕ_0. For exponential and hyperbolic examples, however, it measures the steepness of the potentials as given by $\bar{\phi}$.

Although the value of ϕ_0 is undetermined because of the inherent freedom to shift ϕ by a constant, some information of the range of ϕ covered by observations of the spectra on scales between λ_0 and λ_1 can be recovered. We can start with Eq. (3.13), the reconstruction equation for $\phi(\lambda)$ and find

$$\phi_1 - \phi_0 = \pm\frac{\sqrt{2}}{\kappa}\int_{\lambda_0}^{\lambda_1}\frac{d\lambda'}{\lambda'}\frac{A_S(\lambda')A_G(\lambda')}{A_S^2(\lambda') - A_G^2(\lambda')}, \tag{5.9}$$

where $\phi_1 \equiv \phi(\lambda_1)$. Then, we can then use a simple trapezoidal integration rule to find $\phi_1 - \phi_0$ in terms of the spectra at λ_0 and λ_1.

VI. DETERMINING THE PRIMEVAL SPECTRUM

Conventionally, one chooses a particular theory, assesses the spectrum it predicts and attempts a comparison between its predictions and the observed Universe. For our purposes here, one must be more ambitious and execute this procedure in reverse order, proceeding from the observations to the primeval spectrum, and thence to the underlying inflationary theory. As well as covering the current observational position, we intend to survey the possibilities inherent in future experiments, both proposed and conjectural, in determining the primeval spectrum.[11] In keeping with our inflationary motivation, we assume throughout that we have a universe of critical density.

The range of scales of interest stretches from the present horizon scale, $6000h^{-1}$ Mpc, down to about $1h^{-1}$ Mpc, the scale which contains roughly enough matter to form a typical galaxy.[12] On the microwave sky, an angle of θ (for small enough θ) samples linear scales of $100h^{-1}(\theta/1^\circ)$Mpc.[13] For purposes of discussion, it is convenient to split this range into three separate regions.

- **Large scales: $6000h^{-1}$ Mpc $\longrightarrow$ $\sim 200h^{-1}$ Mpc:**
  These scales entered the horizon after the decoupling of the microwave back-

[11] For an extensive review of large-scale structure studies, see the papers of Efstathiou [29] and Liddle and Lyth [28].

[12] The present density of the Universe is $\rho_0 = 3H_0^2/8\pi G \simeq 2.8h^{-1} \times 10^{11} M_\odot (h^{-1}\mathrm{Mpc})^{-3}$, where $M_\odot$ is the solar mass.

[13] The surface of last scattering is located some $200h^{-1}$ Mpc inside the horizon distance.

ground. Except in models with peculiar matter contents, perturbations on these scales have not been affected by any physical processes, and the spectrum retains its original form. At present the perturbations are still very small, growing in the linear regime without mode coupling. Here, we are still seeing the primeval spectrum.

- **Intermediate scales: $\sim 200h^{-1}$ Mpc $\longrightarrow$ $8h^{-1}$ Mpc:**
  These scales remain in the linear regime, and their gravitational growth is easily calculable. However, they have been seriously influenced by the matter content of the Universe, in a way normally specified by a *transfer function*, which measures the decrease in the density contrast relative to the value it would have had if the primeval spectrum had been unaffected. Even in CDM models, where the only effect is the suppression of growth due to the Universe not being completely matter dominated at the time of horizon entry, this effect is at the 25% level at $200h^{-1}$ Mpc. To reconstruct the primeval spectrum on these scales, it is thus essential to have a strong understanding of the matter content of the Universe, including dark matter, and of its influence on the growth of density perturbations.

- **Small scales: $8h^{-1}$ Mpc $\longrightarrow$ $1h^{-1}$ Mpc:**
  On these scales the density contrast has reached the nonlinear regime, coupling together modes at different wavenumbers, and it is no longer easy to calculate the evolution of the density contrast. This can be attempted either by an approximation scheme such as the Zel'dovich approximation [29,30], or more practically via N–body simulations [31]. Further, hydrodynamic effects associated with the nonlinear behavior can come into play, giving rise to an extremely complex problem with important non-gravitational effects. Again, the transfer function plays a crucial role on these scales. In hot dark matter models, perturbations on these scales are most likely almost completely erased by free streaming, and hence no information can be expected to be available (far less than the rather detailed information reconstruction would require). In a CDM model, enough residual perturbations may remain on these scales for useful information to be obtained.

Let us now consider each range of scales in turn, starting with the largest scales and working down to the smallest scales.

A. Large scales ($6000h^{-1}$ Mpc $\longrightarrow$ $\sim 200h^{-1}$ Mpc):

Without doubt the most important form of observation on large scales for the near future is large-angle microwave background anisotropies. Scales of a couple of degrees or more fall into our definition of large scales. Such measurements are of the purest form available—anisotropy experiments directly measure the gravitational potential

at different parts of the sky, on scales where the spectrum retains its primeval form. Such measurements also are of interest in that the tensor modes may contribute. Tensor modes do not participate in structure formation and most measurements we shall discuss are oblivious to them. Further, tensor modes inside the horizon redshift away relative to matter, and so tensor modes also fail to participate in small-angle microwave background anisotropies.

Nevertheless, these large-scale measurements still exhibit one crucial and ultimately uncircumventable problem. On the largest scales, the number of statistically independent sample measurements that can be made is small. Given that the underlying inflationary fluctuations are stochastic, one obtains only a limited set of realizations from the complete probability distribution function. Such a subset may insufficiently specify the underlying distribution, which is the quantity predicted by an inflationary model, for our purposes. This effect, which has come to be known as the *cosmic variance*, is an important matter of principle, being a source of uncertainty which remains even if perfectly accurate experiments could be carried out. At any stage in the history of the Universe, it is impossible to accurately specify the properties (most significantly the mean, which is what the spectrum specifies assuming gaussian statistics) of the probability distribution function pertaining to perturbations on scales close to that of the observable Universe.

Observations other than microwave background anisotropies appear confined to the long term future. Even such an ambitious project as the Sloan Digital Sky Survey (SDSS) [32] can only reach out to perhaps $500h^{-1}$ Mpc, which can only touch the lower end of our specified large scales. However, in order to specify the fluctuations accurately, one needs many statistically independent regions (100 seems an optimistic lower estimate) which means that the SDSS may not specify the spectrum with sufficient accuracy above perhaps $100h^{-1}$ Mpc.

A much more crucial issue is that the SDSS will measure the galaxy distribution power spectrum, not the mass distribution power spectrum that is our inflationary prediction. In modern work it is taken almost completely for granted that these are not the same, and it seems likely too that a bias parameter (relating the two by a multiplicative constant) which remains scale independent over a wide range of scales may be hopelessly unrealistic. Consequently, converting from the galaxy power spectrum back to that of the matter may require a detailed knowledge of the process of galaxy formation and the environmental factors around distant galaxies. Once one attempts to reach yet further galaxies with a long look-back time, one must also understand something about evolutionary effects on galaxies. As we shall discuss in the section on intermediate scales, it seems likely that peculiar velocity data may be rather more informative than the statistics of the galaxy distribution.

A more useful tool for large scales is microwave background anisotropies on large angular scales. Our formalism closely follows that of Scaramella and Vittorio [33]. On large angular scales, the most convenient tool for studying microwave background

anisotropies is the expansion into spherical harmonics

$$\frac{\Delta T}{T}(\mathbf{x},\theta,\phi) = \sum_{l=2}^{\infty}\sum_{m=-l}^{l} a_{lm}(\mathbf{x})\, Y_m^l(\theta,\phi), \tag{6.1}$$

where θ and ϕ are the usual spherical polars and $\mathbf{x}$ is the observer position. With spherical harmonics defined as in [34], the reality condition is

$$a_{l,-m} = (-1)^m\, a^*_{l,m}. \tag{6.2}$$

In the expansion, the unobservable monopole term has been removed. The dipole term has also been completely subtracted; the intrinsic dipole on the sky cannot be separated from that induced by our peculiar velocity relative to the comoving frame, though it is easy to show that for adiabatic perturbations it will be negligible compared to it.

With gaussian statistics for the density perturbations, the coefficients $a_{lm}(\mathbf{x})$ are gaussian distributed stochastic random variables of position, with zero mean and rotationally invariant variance depending only on l

$$\langle a_{lm}(\mathbf{x})\rangle = 0 \quad ; \quad \langle |a_{lm}(\mathbf{x})|^2\rangle \equiv \Sigma_l^2. \tag{6.3}$$

It is crucial to note that a single observer such as ourselves sees a single realization from the probability distribution for the a_{lm}. The observed multipoles as measured from a single point are defined as

$$Q_l^2 = \frac{1}{4\pi}\sum_{m=-l}^{l} |a_{lm}|^2, \tag{6.4}$$

and indeed the temperature autocorrelation function can be written in terms of these

$$C(\alpha) \equiv \left\langle \frac{\Delta T}{T}(\theta_1,\phi_1)\frac{\Delta T}{T}(\theta_2,\phi_2)\right\rangle_{\alpha} = \sum_{l=2}^{\infty} Q_l^2 P_l(\cos\alpha), \tag{6.5}$$

where the average is over all directions on a single observer sky separated by an angle α, and $P_l(\cos\alpha)$ is a Legendre polynomial. The expectation for the Q_l^2, averaged over all observer positions, is just

$$\langle Q_l^2\rangle = \frac{1}{4\pi}(2l+1)\Sigma_l^2. \tag{6.6}$$

A given model predicts values for the averaged quantities $\langle Q_l^2\rangle$. On large angular scales, corresponding to the lowest harmonics, only the Sachs–Wolfe effect operates. One has two terms corresponding to the scalar and tensor modes—we denote these contributions by square brackets. The scalar term is given by the integral

$$\Sigma_l^2[S] = \frac{8\pi^2}{m^2}\int_0^{\infty}\frac{dk}{k} j_l^2(2k/aH)\,\frac{2}{m^2}\dot{A}_S^2 T^2(k), \tag{6.7}$$

where j_l is a spherical Bessel function and the transfer function $T(k)$ is normalized to one on large scales. As an example, a power-law spectrum $kA_S^2 \propto k^n$ on scales where the transfer function is sufficiently close to unity gives the oft-quoted

$$\Sigma_l^2[S] = \Sigma_2^2[S] \frac{\Gamma(l + (n-1)/2)}{\Gamma(l + (5-n)/2)} \frac{\Gamma((9-n)/2)}{\Gamma((3+n)/2)}, \tag{6.8}$$

which for a flat $n = 1$ spectrum gives the simple $\Sigma_l^2[S] = 6\Sigma_2^2[S]/l(l+1)$. However, true reconstruction requires the integral expression.

The equivalent expression for the tensor modes is a rather complicated multiple integral which usually must be calculated numerically [14,15,20]. Under many circumstances (Lucchin, Matarrese and Mollerach [20] suggest $0.5 < n < 1$ for power-law inflation) there is a helpful approximation which is that the ratio $\Sigma_l^2[S]/\Sigma_l^2[T]$ is independent of l and given by

$$\frac{\Sigma_l^2[S]}{\Sigma_l^2[T]} = \frac{2}{m^2} \frac{A_S^2}{A_G^2}. \tag{6.9}$$

For many purposes this is a perfectly adequate expression, but for true reconstruction of the inflaton potential, one must of course use the exact integral expression.

On the sky, one does not observe each contribution to the multipoles separately. As uncorrelated stochastic variables, the expectations add in quadrature to give

$$\Sigma_l^2 = \Sigma_l^2[S] + \Sigma_l^2[T]. \tag{6.10}$$

For reconstruction purposes, there are two obstructions of principle. These are

- Even if one could measure the Σ_l^2 exactly, the last scattering surface being closed means one obtains only a discrete set of information—a finite number of the Σ_l covering some effective range of scales.[14] There will thus be an uncountably infinite set of possible spectra which predict exactly the same set of Σ_l.

- One cannot measure the Σ_l^2 exactly. What one can measure is a single realization, the Q_l^2. As a sum of $2l+1$ gaussian random variables, Q_l^2 has a probability distribution which is a χ^2 distribution with $2l+1$ degrees of freedom, χ_{2l+1}^2. The variance of this distribution is given by

$$\mathrm{Var}[Q_l^2] = \frac{2}{2l+1} \langle Q_l^2 \rangle^2, \tag{6.11}$$

though one should remember that the distribution is not symmetric. Each Q_l^2 is a single realization from that distribution, when we really want to know the mean. From a single observer point, there is no way of obtaining that mean, and

[14]The l-th multipole is often taken as corresponding roughly to a scale $k_l \simeq lH_0/2\mathrm{Mpc}^{-1} = lh/6000\mathrm{Mpc}^{-1}$.

one can only draw statistical conclusions based on what can be measured. Thus, a larger set of spectra which give different sets of Σ_l^2 can still give statistically indistinguishable sets of Q_l^2. The variance falls with increasing l but is significant right across the range of large scales. This is illustrated in Figure 2.

Finally, it should be mentioned that measurements of the polarization of the CMBR on large scales may allow a separate determination of the gravitational wave spectrum to be made [35]. Such an effect is potentially detectable if gravitational waves dominate the *COBE* result and the polarization is of the order of 10%, say. If the waves only contribute 10% of the *COBE* signal, for example, then only 10% of 10% is polarized, which significantly reduces the overall effect. Unfortunately, reconstruction of the potential must await a positive detection of such an effect, so we will not discuss it further.

B. Intermediate scales ($\sim 200h^{-1}$ Mpc $\longrightarrow 8h^{-1}$ Mpc)

It is on intermediate scales that determination of the primeval spectrum is most promising, though sadly these scales only encompass about 3 e-foldings. Here a range of promising observations are available, particularly towards the small end of the range of scales. In terms of technical difficulties in interpreting measurements, a trade-off has been made compared to large scales; on the plus side, the cosmic variance is a much less important player as far more independent samples are available, while on the minus side the spectrum has been severely affected by physical processes and thus has moved a step away from its primeval form.[15]

1. Intermediate-scale microwave background anisotropies

In the absence of reionization, the relevant angular scales are from about 2° down to about 5 arcminutes. (Should reionization occur, a lot of the information on these scales could be erased or amended in difficult to calculate ways.) Several experiments are active in this range, including the South Pole and MAX experiments, but as none have yet published a positive detection they are not of direct interest to us here at present. Indeed, even with a detection many of these ground based experiments are unable to give results with the statistical quality we would require due to the small sky coverage which is typically involved.

Unlike the large-scale anisotropy, one cannot write down a simple expression for the intermediate-scale anisotropies, even if it is assumed that one has already incorporated the effect of dark matter on the growth of perturbations via a transfer function.

[15] In the distant future, when the horizon size is vastly greater than at the present, there will be a range of scales above $200h^{-1}$ Mpc where the cosmic variance remains small and the spectrum retains it primeval form. Such a region would be an ideal place to carry out reconstruction, but unfortunately does not exist at the present epoch.

The reason is due to the complexity of physical processes operating. A case in point is the expected anisotropy (specified by the Σ_l^2, but now for larger l) in the CDM model ($n = 1$), as calculated in detail by Bond and Efstathiou [36].

On large scales, $l^2\Sigma_l^2$ is approximately independent of l as we have seen. Once we get into the intermediate regime, $l^2\Sigma_l^2$ exhibits a much more complicated form, which is dominated by a strong peak at around $l = 200$. This is induced by Thomson scattering from moving electrons at the time of recombination. Bond and Efstathiou's calculation gives a peak height around 6 times as high as the extrapolated Sachs–Wolfe effect. Beyond the first peak is a smaller subsidiary peak at $l \sim 800$.

In their calculation, Bond and Efstathiou assumed both the primeval spectrum and the form of the dark matter. For reconstruction purposes, it seems that a good knowledge of the form of dark matter is a pre-requisite, in order that these processes can be calculated at all. Of course, given the number of active and proposed dark matter search experiments, one should be optimistic that this information will be obtained in the not too distant future. However, even with this information, the complexity of the calculation makes it hard to conceive of a way of inverting it, should a good experimental knowledge of the Σ_l^2 ($l \in [30, 750]$) be obtained. Once again, it's much easier to compare a given theory with observation than to extract a theory from observation.

One of the interesting applications of these results might be in combination with the large-scale measurements. The peak on intermediate scales is due only to processes affecting the scalar modes, whereas we have pointed out that the large-scale Sachs–Wolfe effect is a combination of scalar and tensor modes. On large scales, one cannot immediately discover the relative normalizations of the two contributions. However, if the dark matter is sufficiently well understood, the height of the peak in the intermediate regime gives this information. Should it prove that the tensors do play a significant role, then this would be a very interesting result as it immediately excludes slow-roll potentials for the regime corresponding to the largest scales. Should the tensors prove negligible, then although the conclusions are less dramatic one has an easier inversion problem on large scales as one can concentrate solely on scalar modes.

2. Galaxy clustering in the optical and infrared

A. Redshift surveys in the optical.

Over the last decade, enormous leaps have been made in our understanding of the distribution of galaxies in the Universe from various redshift surveys. Most prominent is doubtless the ongoing Center for Astrophysics (CfA) survey [37], which aims to form a complete catalogue of galaxy redshifts out to around $100h^{-1}$ Mpc. Other surveys of optical galaxies, often trading incompleteness for greater survey depth, are also in progress. On the horizon is the Sloan Digital Sky Survey [32] which aims to find the redshifts of one million galaxies, occupying one quarter of the sky, with an overall

depth of $500h^{-1}$ Mpc and completeness out to $100h^{-1}$ Mpc.

The redshifts of galaxies are relatively easy (though time consuming) to measure and interpret, and so provide one of the more observationally simple means of determining the distribution of matter in the Universe. The main technical problem is to correct the distribution for redshift distortions (which gives rise to the famous "fingers of God" effect). However, the distribution of galaxies, specified by the galaxy power spectrum (or correlation function) is two steps away from telling us about the primeval mass spectrum.

- We have already discussed that the primeval spectrum on intermediate scales has been distorted by a combination of matter dynamics and amendments to the perturbation growth rate when the Universe is not completely matter dominated. If we know what the dark matter is, then this need not be a serious problem.

- Galaxies need not trace mass, and in modern cosmology it is almost always assumed they do not. This makes the process of getting from the galaxy power spectrum to the mass power spectrum extremely non-trivial. Models such as biased CDM rely on the notion of a scale-independent ratio between the two, but this too can only be an approximation to reality. In recent work, authors have emphasised the possible influence of environmental effects on galaxy formation (for instance, a nearby quasar might inhibit galaxy formation [38]), and indeed it has been demonstrated that only very modest effects are required in order to profoundly affect the shapes of measured quantities such as the galaxy angular correlation function [39].

Despite this, attempts have been made to reconstruct the power spectrum from various surveys. In particular, this has been done for the CfA survey [40], and for the Southern Sky Redshift Survey [41]. These reconstructions remain very noisy, especially at both large scales (poor sampling) and small scales (shot noise and redshift distortions), and at present the best one could do would be to try and fit simple functional forms such as power-laws or parametrized power spectra to them. Even then, the constraints one would get on the slope of say a tilted CDM spectrum are very weak indeed. However, these reconstructions go along with the usual claim that standard CDM is excluded at high confidence due to inadequate large-scale clustering, without providing any particular constraints on the choice of methods of resolving this conflict.

Nevertheless, with larger sampling volumes such as those which the SDSS will possess, one should be able to get a good determination of the *galaxy* power spectrum across a reasonable range of scales, perhaps $10h^{-1}$ to $100h^{-1}$ Mpc.

B. Redshift surveys in the infrared.

A rival to redshifts of optical galaxies is those of infra-red galaxies, based on galaxy positions catalogued by the Infra-Red Astronomical Satellite (IRAS) project

in the mid-eighties. The aim here is to sparse-sample these galaxies and redshift the subset. This is being done by two groups, giving rise to the QDOT survey [42] and the 1.2 Jansky survey [43]. Taking advantage of the pre-existing data-base of galaxy positions has allowed these surveys to achieve great depth with even sampling and reach some interesting conclusions.

The main obstacle to comparison with optical surveys is due to the selection method. Infra-red galaxies are generally young, and appear to possess a distribution notably less clustered than their optically selected counterparts. They are thus usually attributed their own bias parameter which differs from the optical bias. The mechanics of proceeding to the power spectrum are basically the same as for optical galaxies.

The most interesting and relevant results here are obtained in combination with peculiar velocity information, as discussed below.

C. Projected catalogues.

As well as redshift surveys, one also has surveys which plot the positions of galaxies on the celestial sphere. At present the most dramatic is the APM survey [44], encompassing several million galaxies. The measured quantity is the projected counterpart of the correlation function, the angular correlation function usually denoted $w(\theta)$ where θ is the angular separation. Though arguments remain as to the presence of systematics, one in principle has accurate determinations of the galaxy angular correlation function. The first aim is to reconstruct the full three dimensional correlation function from this (proceeding thence to the galaxy power spectrum). Unfortunately, present methods of carrying out this inversion (based on inverting Limber's equation which gives $w(\theta)$ from $\xi(r)$) have proven to be very unstable, and a satisfactory recovery of the full correlation function has not been achieved.

In its preliminary galaxy identification stage, the SDSS will provide a huge projected catalogue on which further work can be carried out.

3. Peculiar velocity flows

Potentially the most important measurements in large-scale structure are those of the peculiar velocity field. Because all matter participates gravitationally, peculiar velocities directly sample the mass spectrum, not the galaxy spectrum. Were one to know the peculiar velocity field, this information is therefore as close to the primeval spectrum as is microwave background information. Indeed, in the linear regime the spectrum of the modulus v of the velocity[16] is just given by

$$\mathcal{P}_v(k) = \frac{1}{25\pi}\left(\frac{aH}{k}\right)^2 \frac{2}{m^2} A_S^2(k) T^2(k). \tag{6.12}$$

[16]The spectrum is defined as $\mathcal{P}_v = V(k^3/2\pi^2)(|\delta_v|^2)$, with V being the volume over which the Fourier components $\delta_v(k)$ are defined.

Perhaps the most exciting recent development in peculiar velocity observations is the development of the POTENT method by Bertschinger, Dekel and collaborators [45]. Using only the assumption that the velocity can be written as the divergence of a scalar (in gravitational instability theories in the linear regime this is naturally associated with the peculiar gravitational potential), they demonstrate that the radial velocity towards/away from our galaxy (which is all that can be measured by the methods available) can be used to reconstruct the scalar, which can then be used to obtain the full three dimensional velocity field. This has been shown to work very well in simulated data sets, where one mimics observations and then can compare the reconstruction from those measurements with the original data set. So far, the noisiness and sparseness of available real radial velocity data has meant that attempts to reconstruct the fields in the neighborhood of our galaxy have not yet met with great success; however, once better and more extensive observational data are obtained one can expect this method to yield excellent results.

At present, POTENT appears at its most powerful in combination with a substantial redshift survey such as the IRAS/QDOT survey. As POTENT supplies information as to the density field and the redshift survey to the galaxy distribution, the two in combination can be used in an attempt to measure quantities such as the bias parameter and the density parameter Ω_0 of the Universe. Reconstructions of the power spectrum have also been attempted [46]. At present, the error bars (due to cosmic variance because of small-sampling volume, due to the sparseness of the data in some regions of the sky and due to iterative instabilities) are large enough that a broad range of spectra (including standard CDM) are compatible with the reconstructed present-day spectrum.

With larger data sets and technical developments in the theoretical analysis tools, POTENT (and indeed velocity data in general) appears to be a very powerful means of investigating the present-day power spectrum. To that, one need only add a knowledge of the dark matter to obtain the primeval spectrum and thence to the inflaton potential. Although likely to be limited to the range of scales specified at the lower end by the onset of the nonlinear regime and at the upper end by the range of feasible experimental measurements of the radial peculiar velocity, it seems that velocity data provide the most promising means of reconstructing a segment of the inflaton potential.

C. Small scales ($8h^{-1}$ Mpc $\longrightarrow$ $1h^{-1}$ Mpc):

It is worth saying immediately that this promises to be the least useful range of scales. For many choices of dark matter, including the standard hot dark matter scenario, perturbations on these scales are almost completely erased by dark matter free-streaming to leave no information as to the primeval spectrum. Only if the dark matter is cold does it seem likely that any useful information can be obtained.

There are several types of measurement which can be made. Quite a bit is known

about galaxy clustering on small scales, such as the two-point galaxy correlation function. However, the strong nonlinearity of the density distribution on these scales erases information about the original linear-regime structure, and the requirement of N-body simulations to make theoretical predictions makes this an unpromising avenue for reconstruction even should nature have chosen to leave significant spectral power on these scales. There exist very small-scale (arcsecond–arcminute) microwave background anisotropy measurements [47], though these are susceptible to a number of line of sight effects, and further the anisotropies are suppressed (exponentially) on short scales because the finite thickness (about $7h^{-1}$ Mpc) of the last scattering surface comes into play.

Up to now, the most useful constraints on small scales have come from the pairwise velocity dispersion [48] (the dispersion of line-of-sight velocities between galaxies). These are sensitive to the normalization of the spectrum at small scales, though unfortunately susceptible to power feeding down from higher scales as well. There are certainly noteworthy constraints—for instance it is generally accepted that unbiassed standard CDM generates excessively large dispersions. However, the calculations required involve N-body simulations and because a wide range of wavelengths contribute, obtaining knowledge of any structure in the power spectrum on these scales is likely to prove impossible, even if the amplitude can be determined to reasonable accuracy.

VII. DISCUSSION AND CONCLUSIONS

To date, the traditional approach in cosmology has been to take a set of theoretical predictions for the structure of our universe and compare them directly with what is observed. The aim is to reduce to a minimum the space of possible theories consistent with observations. Unfortunately such an analysis can only deduce which theories are unsuitable and is unlikely to select uniquely the correct one. An alternative and more ambitious program is to use the observations to reconstruct the theory. Within the context of the inflationary universe, for example, such an approach is justified when one considers the prize on offer—the form of the inflaton potential. The purpose of the present work has been to illustrate how such a reconstruction of the potential is possible in principle.

There are two steps to any reconstruction procedure. In practice the observational information may not be in a form which allows a direct comparison with the theoretical predictions to be made. It is therefore necessary to first convert the data into the quantity predicted and only then can the second step of reconstructing the potential be completed. As was shown in Section VI, this is especially true in the inflationary universe and presents a number of fundamental difficulties with the procedure.

In Section III, however, we successfully completed the second step of the process

by deriving the correspondences between the tensor and scalar fluctuation spectra and the potential. This extended the analysis of Ref. [7] and a number of examples were presented in Section IV. In a true reconstruction one should make no assumptions concerning the form of the potential. In particular, the assumptions of slow-roll, which are essentially conditions on the flatness of $V(\phi)$, should be avoided. The formalism used places no restrictions on the inflaton field dynamics, but does assume the slow-roll expressions for the perturbation spectra still apply. From a computational point of view, it follows that reconstruction is unambiguous once the t[illegible]ctrum is known. Unfortunately, however, it is this quantity which is the [illegible] difficult to determine observationally. The only observational effect of primordial gravitational waves appears to be their influence on large-scale CMBR anisotropies. We conclude that the most promising method of determining the tensor spectrum is to combine the large-scale CMBR results with intermediate scale data from peculiar velocities and CMBR anisotropies. The latter require a knowledge of the dark matter component, but are independent of any bias in the galaxy distribution. They determine the scalar spectrum, whereas the former depends on both the scalar and tensor modes. A simple subtraction therefore yields the tensor spectrum.

Eq. (3.11) will allow a test of the inflationary paradigm to be made if a separate determination of the tensor spectrum on large scales can be made. A separate determination of A_G on large angular scales coupled with *COBE* [1], Tenerife [49] and the Princeton-MIT balloon [50] would lead to A_S^2. This could then be compared with the theoretical prediction derived from Eq. (3.11). If a discrepancy was found, it would suggest that one or more of the initial assumptions—such as the background spacetime being flat; using a single, minimally coupled scalar field or Einstein gravity—were incorrect. On the other hand, in the absence of any discrepancy, this result could be used with a combination of CMBR measurements around 2°, velocity and galaxy clustering data, and compared with the theoretical predictions for different dark matter models. This would lead to limits on the form of dark matter present in the Universe.

We note that reconstruction is still possible if the gravitational waves are not significant, although one must then deal with the integration constant which arises in the solution of Eq. (3.11) and can affect the functional form of the potential.

Although we have been somewhat pessimistic about the near-term prospects for reconstructing the functional form of the potential, we are optimistic regarding the near-term possibility of obtaining some knowledge about the potential. To illustrate the promise of our method, let us *assume* that within a few years that a combination of CMBR measurements give us some information about the scalar and tensor amplitudes at a particular length scale λ_0 (corresponding to an angular scale θ_0). An example is that we might in the near future have in hand the following:

$$A_S(\lambda_0) = 1 \times 10^{-5}; \qquad A_G(\lambda_0) = 2 \times 10^{-6}; \qquad n_0 = 0.9; \qquad n_0' = 0. \qquad (7.1)$$

If we would have this information, we can follow the perturbative procedure outlined in Section V and reconstruct information about the potential in the vicinity of

some point ϕ_0:

$$\begin{aligned} V(\phi_0) &= (2 \times 10^{16}\mathrm{GeV})^4 \\ \pm V'(\phi_0) &= (3 \times 10^{15}\mathrm{GeV})^3 \\ V''(\phi_0) &= (5 \times 10^{13}\mathrm{GeV})^2. \end{aligned} \tag{7.2}$$

By taking some appropriate ratios one may find mass scales for the potential. In this way cosmology might be first to get a "piece of the action" of GUT–scale physics.

ACKNOWLEDGMENTS

EJC and ARL are supported by the Science and Engineering Research Council (SERC) UK. JEL is supported by an SERC postdoctoral research fellowship. EWK and JEL are supported at Fermilab by the DOE and NASA under Grant NAGW–2381. ARL acknowledges the use of the Starlink computer system at the University of Sussex. We would like to thank D. Lyth, P. J. Steinhardt, and M. S. Turner for helpful discussions.

References

1. G. F. Smoot *et al*, *Astrophys. J. Lett.* **396**, L1 (1992); E. L. Wright *et al*, *Astrophys. J. Lett.* **396**, L13 (1992).

2. R. K. Sachs and A. M. Wolfe, *Astrophys. J.* **147**, 73 (1967); P. J. E. Peebles, *Astrophys. J. Lett.* **263**, L1 (1982).

3. A. Guth, *Phys. Rev. D* **23**, 347 (1981).

4. D. La and P. J. Steinhardt, *Phys. Rev. Lett.* **62**, 376 (1989); E. W. Kolb, D. S. Salopek and M. S. Turner, *Phys. Rev. D* **42**, 3925 (1990); E. W. Kolb, *Physica Scripta* **T36**, 199 (1991); J. E. Lidsey, *Class. Quantum Grav.* **9** (1992) 149; J. E. Lidsey, Ph. D. Thesis, London University (1992); A. H. Guth and B. Jain, *Phys. Rev. D* **45**, 441 (1992).

5. A. Albrecht and P. J. Steinhardt, *Phys. Rev. Lett.* **48**, 1220 (1982); A. D. Linde, *Phys. Lett.* **108B**, 389 (1982).

6. A. D. Linde, *Phys. Lett.* **129B**, 177 (1983).

7. H. M. Hodges and G. R. Blumenthal, *Phys. Rev. D* **42**, 3329 (1990).

8. J. M. Bardeen, *Phys. Rev. D* **22**, 1882 (1980).

9. J. E. Lidsey, *Phys. Lett.* **273B**, 42 (1991).

10. F. Lucchin and S. Matarrese, *Phys. Rev. D* **32**, 1316 (1985); *Phys. Lett.* **164B**, 282 (1985).

11. P. J. Steinhardt and M. S. Turner, *Phys. Rev. D* **29**, 2162 (1984); E. W. Kolb and M. S. Turner, *The Early Universe*, (Addison-Wesley, New York, 1990).

12. A. R. Liddle and D. H. Lyth, *Phys. Lett.* **291B**, 391 (1992).

13. T. Bunch and P. C. W. Davies, *Proc. Roy. Soc. London* **A360**, 117 (1978).

14. L. F. Abbott and M. B. Wise, *Nucl. Phys.* **B244**, 541 (1984).

15. A. A. Starobinsky, *Sov. Astron. Lett.* **11**, 133 (1985).

16. V. Belinsky, L. Grischuk, I. Khalatanikov and Ya. B. Zel'dovich, *Phys. Lett.* **155B**, 232 (1985).

17. B. J. Carr and J. E. Lidsey, "Primordial Black Holes and Generalized Constraints on Chaotic Inflation," QMW preprint (1993).

18. L. M. Krauss and M. White, *Phys. Rev. Lett.* **69**, 869 (1992); J. E. Lidsey and P. Coles, *Mon. Not. Roy. astr. Soc.* **258**, 57P (1992); D. S . Salopek, *Phys. Rev. Lett.* **69**, 3602 (1992); D. S. Salopek, in *Proceedings of the International School of Astrophysics "D. Chalogne" second course*, ed N. Sanchez (World Scientific, 1992); T. Souradeep and V. Sahni, *Mod. Phys. Lett.* **A7**, 3541 (1992); M. White, *Phys. Rev. D* **46**, 4198 (1992); R. Crittenden, J. R. Bond, R. L. Davis, G. Efstathiou and P. J. Steinhardt, in *Proceedings of the Texas/Pascos Symposium, Berkeley* (1992).

19. R. L. Davis, H. M. Hodges, G. F. Smoot, P. J. Steinhardt and M. S. Turner, *Phys. Rev. Lett.* **69**, 1856 (1992).

20. F. Lucchin, S. Matarrese, and S. Mollerach, *Astrophys. J. Lett.* **401**, 49 (1992).

21. D. H. Lyth and E. D. Stewart, "A More Accurate Analytical Calculation of the Spectrum of Density Perturbations Produced During Inflation," to appear *Phys. Lett.* **B** (1993).

22. D. H. Lyth and E. D. Stewart, *Phys. Lett.* **274B**, 168 (1992).

23. M. S. Turner, "On the Production of Scalar and Tensor Perturbations in Inflationary Models," Fermilab preprint FNAL-PUB-93/026-A (1993).

24. J. E. Lidsey and R. K. Tavakol, "On the Correspondence between Theory and Observation in Inflationary Cosmology," Fermilab preprint FNAL-PUB-93/034-A (1993).

25. K. Freese, J. A. Frieman and A. Olinto, *Phys. Rev. Lett.* **67**, 3233 (1990); F. C. Adams, J. R. Bond, K. Freese, J. A. Frieman and A. V. Olinto, *Phys. Rev. D* **47**, 426 (1993).

26. J. D. Barrow, *Phys. Lett.* **235B**, 40 (1990); J. D. Barrow and A. R. Liddle, "Perturbation Spectra from Intermediate Inflation," Sussex preprint SUSSEX-AST 93/2-1 (1993).

27. E. Witten, *Nucl. Phys.* **B202**, 253 (1980).

28. A. R. Liddle and D. H. Lyth, "The Cold Dark Matter Density Perturbation," to be published, *Phys. Rep.* (1993).

29. G. Efstathiou in *The Physics of the Early Universe*, eds. A. Heavens, J. Peacock and A. Davies, SUSSP publications 1990.

30. Ya. B. Zel'dovich, *Astron. Astrophys.* **5**, 84 (1970).

31. See M. Davis, G. Efstathiou, C. S. Frenk and S. D. M. White, *Nature* **356**, 489 (1992) and refs therein.

32. J. E. Gunn and G. R. Knapp, "The Sloan Digital Sky Survey," Princeton preprint POP-488 (1992); R. G. Kron in *ESO Conference on Progress in Telescope and Instrumentation Technologies*, ESO conference and workshop proceeding no. 42, p635, ed. M.-H. Ulrich (1992).

33. R. Scaramella and N. Vittorio, *Astrophys. J.* **353**, 372 (1990).

34. W. H. Press, B. P. Flannery, S. A. Teukolsky and W. T. Vetterling, *Numerical Recipes*, Cambridge University Press 1986.

35. A. G. Polnarev, *Sov. Astron.* **29**, 607 (1985).

36. J. R. Bond and G. Efstathiou, *Mon. Not. R. astr. Soc.* **226**, 655 (1987).

37. M. J. Geller and J. P. Huchra, *Science* **246**, 879 (1989); M. Ramella, M. J. Geller and J. P. Huchra, *Astrophys. J.* **384**, 396 (1992).

38. A. Babul and S. D. M. White, *Mon. Not. R. astr. Soc.* **253**, 31p (1991).

39. R. G. Bower, P. Coles, C. S. Frenk and S. D. M. White, *Astrophys. J.* **405**, 403 (1993).

40. M. S. Vogeley, C. Park, M. J. Geller and J. P. Huchra, *Astrophys. J. Lett.* **391**, L5 (1992).

41. C. Park, J. R. Gott and L. N. da Costa, *Astrophys. J. Lett.* **392**, L51 (1992).

42. W. Saunders *et al*, *Nature* **349**, 32 (1991); N. Kaiser, G. Efstathiou, R. Ellis, C. Frenk, A. Lawrence, M. Rowan-Robinson and W. Saunders, *Mon. Not. R. astr. Soc.* **252**, 1 (1991).

43. K. B. Fisher, M. Davis, M. A. Strauss, A. Yahil and J. P. Huchra, *Astrophys. J.* **389**, 188 (1992).

44. S. J. Maddox, G. Efstathiou, W. J. Sutherland and J. Loveday, *Mon. Not. R. astr. Soc.* **242**, 43p (1990).

45. E. Bertschinger and A. Dekel, *Astrophys. J. Lett.* **336**, L5 (1989); A. Dekel, E. Bertschinger and S. M. Faber, *Astrophys. J.* **364**, 349 (1990); E. Bertschinger, A. Dekel, S. M. Faber, A. Dressler and D. Burstein, *Astrophys. J.* **364**, 370 (1990).

46. A. Dekel in *Observational Tests of Cosmological Inflation*, eds T. Shanks *et al*, Kluwer Academic 1991.

47. A. C. S. Readhead, C. R. Lawrence, S. T. Myers, W. L. W. Sargent, H. E. Hardebeck and A. T. Moffat, *Astrophys. J.* **346**, 566 (1989).

48. J. M. Gelb, B.-A. Gradwohl and J. A. Frieman, *Astrophys. J. Lett.* **403**, L5 (1993).

49. A. A. Watson *et al*, *Nature* **357**, 660 (1992).

50. S. S. Meyer, E. S. Cheng and L. A. Page, *Astrophys. J. Lett.* **371**, L1 (1991).

51. T. Gaier, J. Schuster, J. Gunderson, T. Koch, M. Seiffert, P. Meinhold and P. Lubin, *Astrophys. J. Lett.* **398**, L1 (1992).

Figure Captions

Figure 1:
A schematic figure illustrating the main concepts behind reconstruction. For inflation the two main steps involve converting the observations (lower half of figure) into the primordial scalar (A_S) and tensor (A_G) fluctuation spectra and then working in reverse to reconstruct the potential $V(\phi)$. The main observational information from the cosmic microwave background arises through the Cosmic Background Explorer (*COBE*) satellite [1], and the Tenerife (TEN) [49] and South Pole (SP) [51] collaborations. Galaxy surveys (APM [44], CfA [37], IRAS [42,43]) may provide useful information up to $100h^{-1}$ Mpc, while the Sloan Digital Sky Survey (SDSS) [32] should extend to the lowest scales measured by *COBE*. Peculiar velocity measurements using the POTENT (P) [45] methods are important on intermediate scales. The angle θ measures angular scales on the CMBR in degrees, and length scales λ are in units of h^{-1} Mpc. d_H refers to the horizon size today and at recombination and $d_{\rm NL} \approx 8h^{-1}$ Mpc is the scale of non-linearity. (See the text for details). Perfect observations will only reconstruct a small portion of the inflaton potential corresponding to between $53 \leq \Delta N \leq 60$ e-foldings before the end of inflation.

Figure 2:
Multipoles up to $l = 30$, roughly corresponding to the complete range of large scales. The solid line represents the ensemble averaged $\langle Q_l^2 \rangle$ (multiplied by l) for a flat ($n = 1$) spectrum of scalar density perturbations with $A_G(\lambda) \ll A_S(\lambda)$, normalized to $\Sigma_2^2 = 1$. The three dashed lines represent different randomly chosen realizations of this distribution. Observations can only supply one such line, giving little clue to the ensemble average quantity that inflation supplies the form of. For comparison, the dash-dotted line shows the result of a scalar spectrum with $n = 0.8$, again with $A_G(\lambda) \ll A_S(\lambda)$ (such a combination would arise from an appropriate inverted harmonic oscillator potential). Note that the normalization of this line is arbitrary (shown here with $\Sigma_2^2 = 1$), and were it moved up it could match an observed distribution across much of the range. More significantly, it is easy to note that any detailed information in the spectrum such as peaks or troughs can be swamped completely by the cosmic variance.

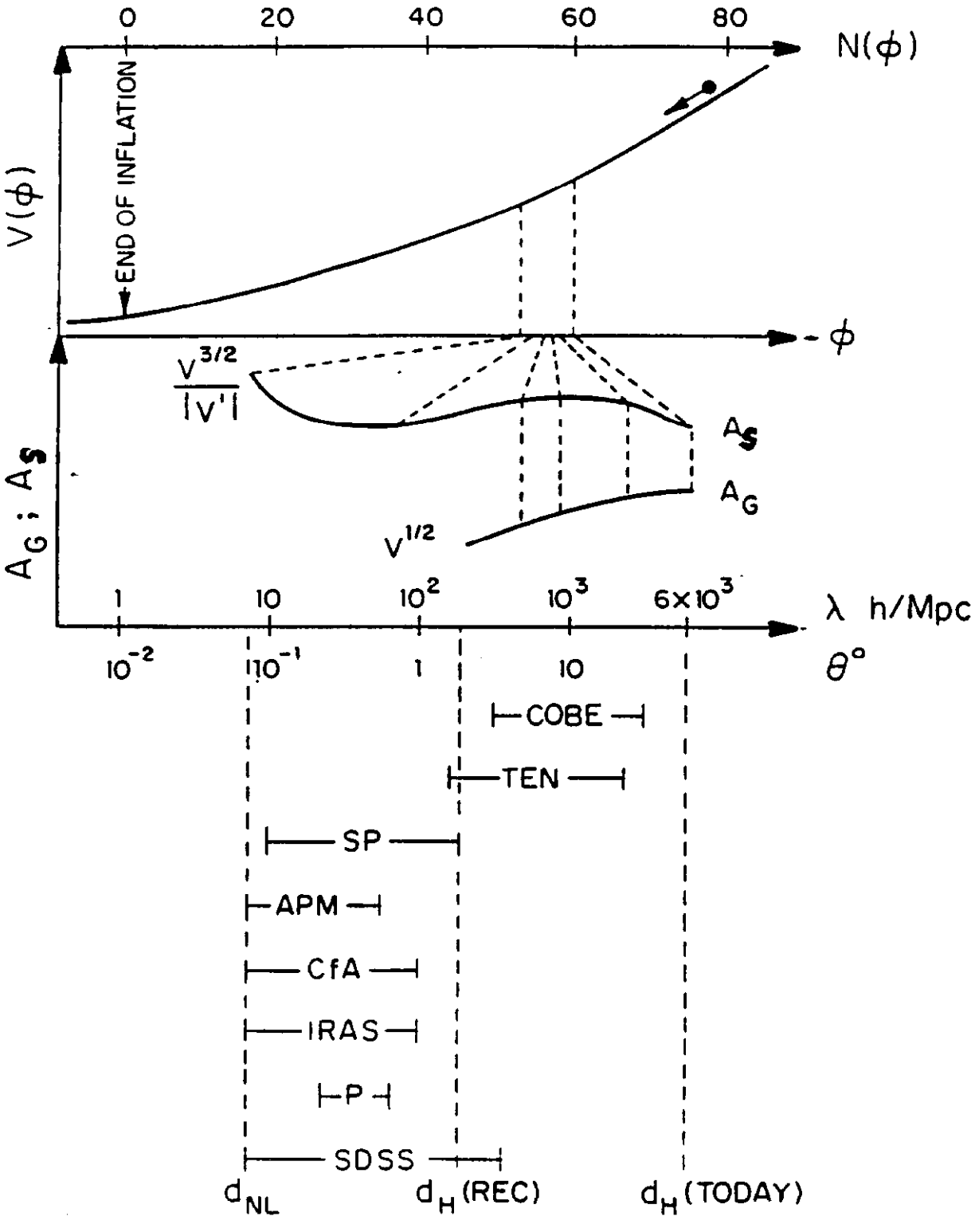
0
20
40
60
80
N(φ)
END OF INFLATION
V(φ)
φ
V^{3/2}/|V'|
A_S
A_G
A_G ; A_S
V^{1/2}
1
10
10^2
10^3
6×10^3
λ h/Mpc
10^{-2}
10^{-1}
1
10
θ°
COBE
TEN
SP
APM
CfA
IRAS
P
SDSS
d_NL
d_H (REC)
d_H (TODAY)

FIGURE 1

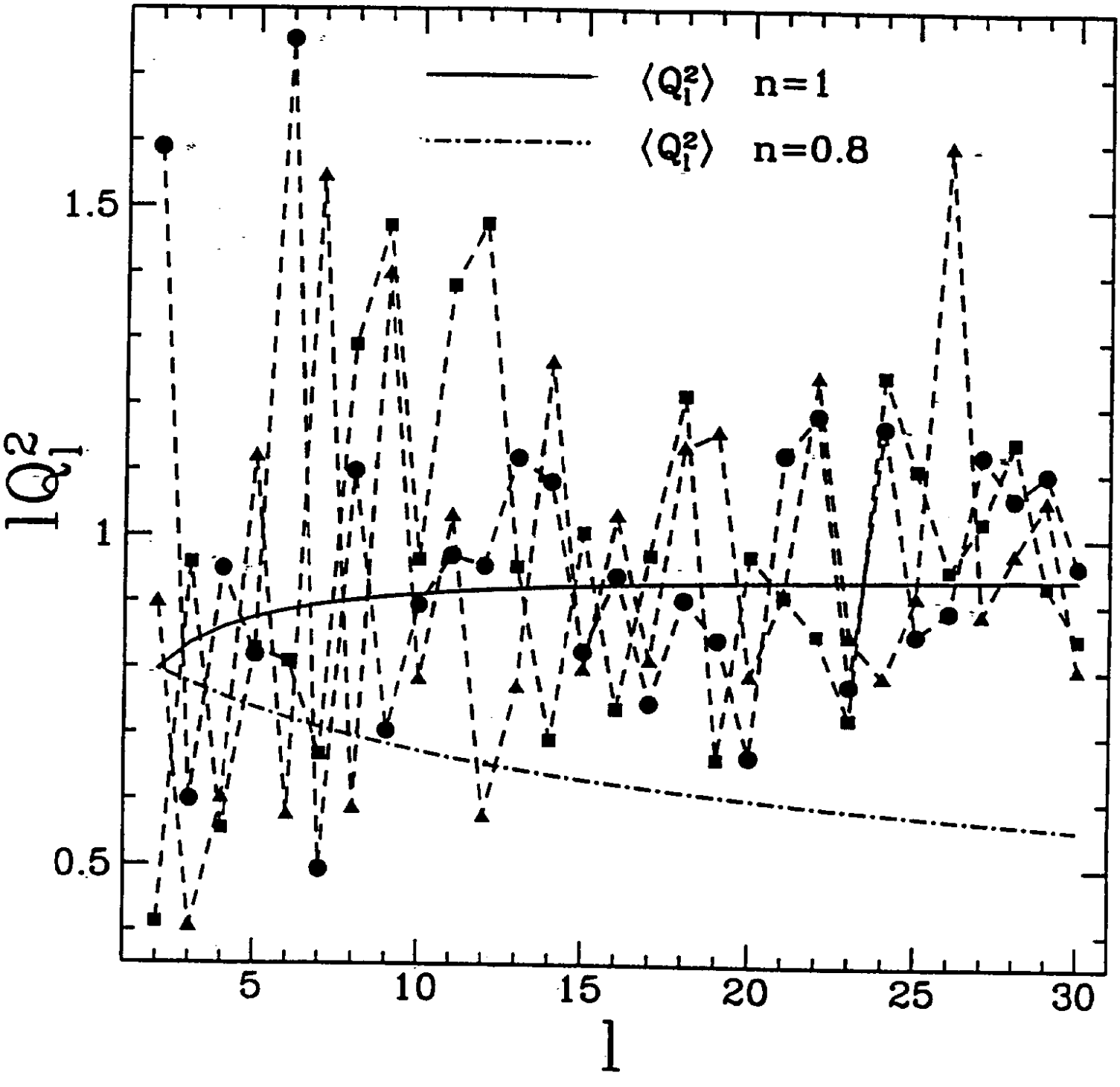
$\langle Q_l^2 \rangle$ n=1
$\langle Q_l^2 \rangle$ n=0.8
lQ_l^2
1.5
1
0.5
5
10
15
20
25
30
l

FIGURE 2